Filter Considerations in Color Correction

Michael J. Vrhel, *Member, IEEE*, and H. Joel Trussell, *Fellow, IEEE*

***Abstract*—The quality of color correction is dependent on the filters used to scan the image. This paper introduces a method of selecting the color filters using *a priori* information about the viewing illuminants. Color correction results using the derived filters are compared with color correction results using filters that are optimal for individual viewing and recording illuminants. The comparison is performed using the CIE $\Delta E_{L^*a^*b^*}$ perceptual color difference measure. Applications of this work are found in the design of scanners, copiers, and television systems.**

I. Introduction

UNDER optimal viewing conditions, it is estimated that the human eye can distinguish 10 million different colors [36]. It is therefore possible, through the use of color, to convey a tremendous amount of information about objects in an image. In many situations, color may be indispensable in interpreting or judging an image. Examples include the following: medical diagnosis [11], the determination of food freshness [37], remote sensing [18], retail catalogs [23], and textile production [24].

In the first step of reproducing a color image, the original image is recorded by measuring the reflected or transmitted energy of the image in a number of different wavelength bands. The illuminant under which an image is recorded—the recording illuminant—will affect the recorded colors. In printing applications, the reproduction will usually be viewed and compared with the original image under an illuminant that is different from the recording illuminant. After the original image is recorded, the data obtained is corrected to compensate for the effects of the recording illuminant, viewing illuminants, and inadequacies in the color filters.

Ideally, the corrected data provides a reproduction device with the information necessary to produce a color match with the original image when the images are compared under a particular viewing illuminant. If any of the colors to be reproduced are outside the color gamut of the display device, then a gamut color correction of the illuminant corrected data is also necessary. The color gamut mapping problem is distinct from the illuminant color correction problem. Illuminant color correction attempts to estimate the exact color the device should reproduce. Color gamut correction involves mapping the colors the reproduction device should ideally reproduce to colors inside the display gamut of the reproduction device [28]. Only the illumination color correction problem will be investigated in this paper.

Manuscript received June 4, 1992; revised March 11, 1993. The associate editor coordinating the review of this paper and approving it for publication was Dr. Fredrick Mintzer.

The authors are with the Electrical and Computer Engineering Department, North Carolina State University, Raleigh, NC 27695-7911.

IEEE Log Number 9215222.

A color copier is an example of a device with a recording illuminant that is different from standard viewing illuminants. For each color filter in the copier, a scan of the image is performed. The recorded data is a function of the recording illuminant, the color filters, the system noise, the sensor response, and the image being recorded. A color copier produces an image by placing varying densities of cyan, magenta, yellow, and black toner onto paper. From the data obtained in the recording process, the copier computes the toner densities necessary to obtain a color match with the original image. The color match will be dependent on the illuminant under which the images are compared. For each viewing illuminant, a different transformation of the recorded data is necessary to obtain a color match. To obtain high-quality color matches between the original image and the reproduction, the recorded data should contain colorimetric information about the original image under the viewing illuminants. *A priori* information about these viewing illuminants can be incorporated into the design of color filters and recording illuminants to reduce color differences between the reproduction and the original image.

In this paper, three approaches of selecting color filters and recording illuminants for color correction are introduced. The first approach uses only knowledge about the radiant spectra of the viewing illuminants. A set of filters that minimizes the maximum square error in a normalized tristimulus space is selected. The second and third approaches use knowledge about the radiant spectra of the viewing illuminants along with statistical information about the reflectance spectra in the image to be recorded. In the second approach, a set of color filters that minimizes the mean square error in a normalized tristimulus space is analytically calculated. In the third approach, a numerical method is used to calculate a set of filters that minimizes a perceptual color error.

II. Mathematical Background

Vector space approaches to color systems have been effectively used to solve problems in color systems [5]-[7], [12], [19], [30], [32], [33]. In a vector space approach, the visible spectrum (400–700 nm) is sampled at N wavelengths. The visible spectrum should be sampled finely enough such that the integration occurring in the recording process can be accurately approximated numerically. The spectral reflectance or spectral transmittance of an object can be represented by an N element vector $\mathbf{f}$. If the spectral power distribution of the illumination is written as an $N \times N$ diagonal matrix $\mathbf{L}$, then the radiant power reflected or transmitted by the object is represented by the vector $\mathbf{Lf}$.

The recording of a color stimulus is performed by measuring the intensity of filtered light. If $\mathbf{n}_i$ represents the transmittance

1057-7149/94$04.00

of filter i, then the recording process can be modeled as

$$\mathbf{c} = \mathbf{N}^T\mathbf{L}_r\mathbf{f} + \mathbf{u} \tag{1}$$

where $\mathbf{N} = [\mathbf{n}_1,\ \mathbf{n}_2,\ \ldots\ \mathbf{n}_P]$, $\mathbf{L}_r$ is the recording illuminant, $\mathbf{c}$ is the P-stimulus value recorded for spectral reflectance $\mathbf{f}$ under illuminant $\mathbf{L}_r$, and $\mathbf{u}$ is additive noise. The ith element of $\mathbf{c}$ approximates the integrated power that passes through the ith color filter. Three color filters are often used, in which case, $\mathbf{c}$ is referred to as a tristimulus value. In practice, the sensor that performs the integration of the filtered light will be nonlinear and have a characteristic spectral sensitivity [2], [10]. The spectral sensitivity response of the sensors can be combined with the transmittance of the color filters to give an overall system spectral sensitivity. For this work, it will be assumed that the brightness of the image and illuminant are such that the device is operating in its linear region.

There are color imaging devices that use a number of recording illuminants in place of color filters to achieve color separation. These devices can also be modeled using (1), where the columns of matrix $\mathbf{N}$ become the spectral power distributions of the recording illuminants, and $\mathbf{L}_r = \mathbf{I}$. We will assume for readability that the imaging device is constructed to have a single illuminant and a number of color filters. The results of this work can be easily adapted to the design of a device with multiple recording illuminants.

The human eye contains four types of sensors consisting of three types of cones, which are used for color vision, and the rods, which are used for low luminance vision. Since this paper concerns color reproduction, it will be assumed that the luminance level is sufficiently high such that only the cone responses need to be considered (see pp. 544–547 of [35] and p. 87 of [15]. The response of the eye to a radiant spectrum $\mathbf{Lf}$ can be represented by

$$\mathbf{r} = \mathbf{C}^T\mathbf{Lf} \tag{2}$$

where the matrix $\mathbf{C} = [\rho, \gamma, \beta]$ contains the sampled spectral sensitivities of the eye sensors. It can be shown that the response of the human visual system to a radiant spectrum is uniquely determined by the orthogonal projection of that radiant spectrum onto the range space of the matrix $\mathbf{C}$ [30]. For this reason, the range space of the matrix $\mathbf{C}$ is defined as the human visual subspace (HVSS). The HVSS can be defined by any set of three vectors that are a nonsingular linear transformation of the column vectors of the matrix $\mathbf{C}$ [30].

To create a standard, the Commission Internationale de l'Eclairage (CIE) calculated a transformation of $\mathbf{C}$, producing a set of nonnegative vectors that are referred to as the CIE XYZ color matching functions. The functions are plotted in Fig. 1. If the sampled CIE XYZ color matching functions are contained in the columns of matrix $\mathbf{A} = [\mathbf{a}_1, \mathbf{a}_2, \mathbf{a}_3]$, then two radiant spectra $\mathbf{g}$ and $\mathbf{h}$ visually match if and only if their tristimulus values are equal

$$\mathbf{A}^T\mathbf{g} = \mathbf{A}^T\mathbf{h}. \tag{3}$$

Illumination color correction transforms the recorded data to obtain the tristimulus values of the original image under a particular illuminant. Mathematically, color correction can be described by

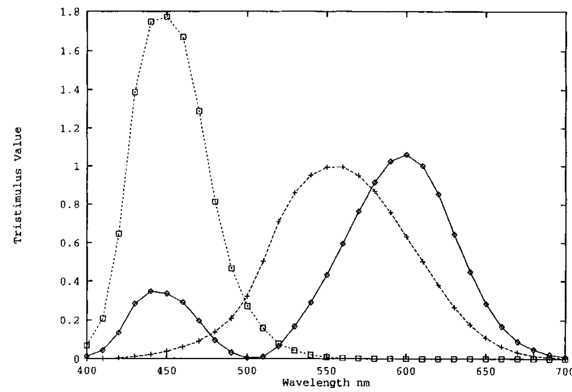

Fig. 1. CIE XYZ color matching functions.

$$\mathcal{P}(\mathbf{c}) = \mathbf{A}^T\mathbf{L}_v\mathbf{f} \tag{4}$$

where $\mathbf{c} = \mathbf{N}^T\mathbf{L}_r\mathbf{f}$ is the recorded data, $\mathbf{L}_v$ is the viewing illuminant, and $\mathcal{P}$ is defined as the ideal color correction transformation. Due to the drastic reduction of information in the recording process, equality can be achieved only under conditions that are rarely met in physical situations.

A linear minimum mean square error (LMMSE) approach to color correction involves the minimization of

$$\epsilon_m = E\{\|\mathbf{t} - \hat{\mathbf{t}}\|^2\} \tag{5}$$

where $\mathbf{t} = \mathbf{A}^T\mathbf{L}_v\mathbf{f}$ and the estimate $\hat{\mathbf{t}}$ is a linear function of the recorded data $\mathbf{c}$

$$\hat{\mathbf{t}} = \mathbf{Wc} + \mathbf{z}\ . \tag{6}$$

The minimization of ϵ_m is performed with respect to $\mathbf{W}$ and $\mathbf{z}$. If the recorded P-stimulus value $\mathbf{c}$ is given by (1) where $\mathbf{u}$ is additive noise uncorrelated with the reflectance spectra, then the LMMSE estimate is

$$\hat{\mathbf{t}} = \mathbf{A^T}\mathbf{L}_v\mathbf{K}_f\mathbf{L}_r\mathbf{N}[\mathbf{N}^T\mathbf{L}_r\mathbf{K}_f\mathbf{L}_r\mathbf{N} + \mathbf{K}_u]^{-1}[\mathbf{c} - \bar{\mathbf{u}} - \mathbf{N}^T\mathbf{L}_r\bar{f}] + \mathbf{A}^T\mathbf{L}_v\bar{\mathbf{f}} \tag{7}$$

where

- $\mathbf{K}_f$ covariance matrix of the reflectance spectra
- $\mathbf{K}_u$ covariance matrix of the noise
- $\bar{\mathbf{f}}$ mean of the reflectance spectra
- $\bar{\mathbf{u}}$ mean of the noise

(see p. 385 of [21]).

The mean square error between the estimated tristimulus value and the actual tristimulus value is not the ideal cost function to minimize since the sensitivity of the eye is not uniform in color spaces which are linear transformations of the HVSS. The minimization of cost functions in color spaces that are more uniform than the CIE tristimulus space are difficult to implement because of the nonlinear transformations involved. An analytical approach is not possible when minimizing with respect to a color metric such as CIE $\Delta E_{L^*a^*b^*}$. Large to intermediate scale nonlinear programming methods are required. An advantage to the LMMSE approach is that the transformation is easily updated for changes in viewing and recording illuminants. A method that requires a numerical solution is not easily updated for changes in illuminations.

III. Selection of Color Filter Subspaces

In many applications, it is desirable to obtain colorimetric information about an object for several viewing illuminants from measurement with a single device. In addition to the color copier example, applications where this would be useful include the textiles industry, in which color variation of dye lots for several illuminants should be closely monitored, and the printing industry, in which accurate color rendition of a product in a retail catalog is important for several illuminants.

There is no discussion in the literature on optimizing color filter subspaces to obtain colorimetric information of a scene under several viewing illuminants. Previous work has recommended selecting P filters that span the same space as the first P principal component vectors of the spectral reflectance covariance matrix [4]. If the goal is spectral reflectance discrimination, then this is a reasonable approach. If the goal is color reproduction, then it is necessary to consider the HVSS in the selection of the filters.

In works that consider the HVSS, the approach has been to design the color scanner such that the filter set spans the HVSS [29], [1]. This is reasonable if the original image and reproduction are to be compared only under a spectrally uniform illumination. If colorimetric information for several viewing illuminants is desired, then filters that span the HVSS do not perform well. The performance of the filters is demonstrated and discussed in Section V.

In remote sensing applications, more than three spectral bands is common. The goal in remote sensing is usually spectral discrimination. The use of more than three filters in the recording process of color images has not been widely discussed in the literature. Kollarits and Gibbon [16] tested the use of five filters for a television application. They achieved a significant improvement in color errors compared with a typical three-filter camera. No optimization was performed with respect to selecting the five filters, and tristimulus values for multiple viewing illuminants were not estimated from the recorded data. In another application, a seven-filter scanner was used to archive art work [20].

It is clear that the color filters used in recording an original image affect the accuracy of any color correction method. In this section, we will pose the problem of obtaining a set of P color filters that improves the accuracy of the color correction method. The HVSS and a particular viewing illuminant $\mathbf{L}_v$ define a 3-D subspace of $\Re^N$. This 3-D subspace is the range space of the matrix $\mathbf{L}_v\mathbf{A}$. If the spectral reflectances in the image are assumed to vary arbitrarily, then, for accurate image reproduction, the color filters/recording illuminant should span the same space as the HVSS under the viewing illuminant. Mathematically, this can be expressed as

$$\mathbf{R}(\mathbf{L}_v\mathbf{A}) = \mathbf{R}(\mathbf{L}_r\mathbf{N}). \tag{8}$$

If the color filters/recording illuminant span the same space as the HVSS under the viewing illuminant, then, in the absence of noise, the desired data can be calculated from the recorded data exactly by a linear transformation. To simplify the notation, the span of the color filters/recording illuminant, which is the spectral sensitivity of the device, will be referred to as the span of the color filters.

Suppose there are two viewing illuminants under which color matches with an original image are desired. In other words, one reproduction should match the original under illuminant $\mathbf{L}_{v_1}$, and a different reproduction should match the original underilluminant $\mathbf{L}_{v_2}$. Both reproductions are to be obtained from the same recorded data. The HVSS combined with the two viewing illuminants defines a subspace of $\Re^N$. The subspace is the range space of the matrix $[\mathbf{L}_{v_1}\mathbf{A}\ \ \mathbf{L}_{v_2}\mathbf{A}]$ and is referred to as the human visual illuminant subspace (HVISS). For the two viewing illuminants case, the dimension of the HVISS could be as large as six. Ideally, the color filters should be selected to span this subspace since the goal is to obtain colorimetric information about the original image under the two viewing illuminants.

This problem can be generalized to K viewing illuminants and P color filters. In this case, the HVSS and the K viewing illuminants define a HVISS with a dimension that could be as large as 3K. If the number of color filters is larger or equal to the dimension of the HVISS, then the filters should be constructed such that the HVISS is in the span of the filters. In this case, the problem becomes one of filter realizability. If the number of color filters is less than the dimension of the HVISS, then the filters cannot span the HVISS. In this case, it is necessary to develop a cost function based on the color correction error, which can be minimized with respect to the color filters.

There is often *a priori* information about the image spectral reflectances that can be used in the design of the color filters. This is especially true if the image to be recorded was produced by a small number of colorants, such as prints produced by four color processes. In applications such as television or still video, *a priori* information about the spectral reflectances may not be available. In this case, an approach of selecting the filter space using only information about the viewing illuminants and the HVSS is useful. Both of these approaches will be addressed in this paper.

A. Approach Using Only Information About Illuminant Spectra

In the case of limited information about the reflectance spectra, the problem of finding a set of optimal filters can be formulated using a min/max method. In the min/max approach, the error to be minimized is

$$\epsilon_l = \underset{\mathbf{f}}{\mathrm{Max}} \sum_{i=1}^{K} \gamma_i^2 \|\mathbf{O}_i^{\mathbf{T}}\mathbf{f} - \mathbf{O}_i^{\mathbf{T}}\hat{\mathbf{f}}\|^2 \tag{9}$$

where the reflectance spectra are assumed arbitrary except that $\|\mathbf{f}\|^2 \leq 1$. The $N \times 3$-dimensional matrices $\mathbf{O}_i \quad i = 1 \ldots K$ are constructed to have orthonormal columns with the range space of $\mathbf{O}_i$ the same as the range space of $\mathbf{L}_{v_i}\mathbf{A}$, where $\mathbf{L}_{v_i} \quad i = 1, \ldots, K$ are the K illuminants under which the reproduction may be viewed. The orthonormalization is performed to remove weightings caused by magnitude differences in the illuminants. The γ_i^2 are used to provide a weighting for the cost of color errors under the various viewing illuminants. Use of the weighting coefficients will be discussed later. The spectral reflectance estimated from the recorded data is $\hat{\mathbf{f}}$. Note that the estimated spectral reflectance $\hat{\mathbf{f}}$ is a function of the color filters since it is calculated from the recorded data.

The optimal filters will depend on the estimation method used to obtain $\hat{\mathbf{f}}$ from the recorded data. To simplify notation, the color filters $\mathbf{N}$ and the recording illuminant $\mathbf{L}_r$ are combined into a single matrix $\mathbf{G}^T = \mathbf{N}^T\mathbf{L}_r$. If the recorded data is given by $\mathbf{c} = \mathbf{N}^T\mathbf{L}_r\mathbf{f}$, then a maximum likelihood estimate (MLE) of the spectral reflectance $\hat{\mathbf{f}}$ is

$$\hat{\mathbf{f}} = (\mathbf{G}^T)^\dagger\mathbf{c} + [\mathbf{I} - (\mathbf{G}^T)^\dagger\mathbf{G}^T]\mathbf{d} \tag{10}$$

where $(\mathbf{G}^T)^\dagger$ is the Moore–Penrose generalized inverse of the matrix $\mathbf{G}^T = \mathbf{N}^T\mathbf{L}_r$ and $\mathbf{d} \in \Re^N$.

Clearly, there is no unique MLE for $\mathbf{f}$. Equation (10) can be rewritten as

$$\hat{\mathbf{f}} = (\mathbf{G}^T)^\dagger\mathbf{c} + \mathbf{v} \tag{11}$$

where $\mathbf{v}$ is any vector in the null space of the matrix $\mathbf{N}^T\mathbf{L}_r$.

A priori knowledge about the reflectance spectra can be used to select $\mathbf{v}$ to improve the estimate of $\mathbf{f}$. For example, reflectance spectra are physically bounded between 0 and 1 and are usually smoothly varying functions of wavelength. The vector $(\mathbf{G}^T)^\dagger\mathbf{c}$ is not guaranteed to be bounded between 0 and 1 nor is it necessarily a smooth function of wavelength. Incorporating these physical constraints into the estimator would complicate the estimation process since set theoretic estimation or constrained quadratic programming becomes necessary. These methods are not realistic for most desktop color imaging applications. For this work, $\hat{\mathbf{f}}$ will refer to the MLE that uses only the data obtained from the color filters. In this case, it is common to select $\hat{\mathbf{f}} = (\mathbf{G}^T)^\dagger\mathbf{c}$—the minimum norm solution—which is the orthogonal projection of the spectral reflectance $\mathbf{f}$ onto the range space of the matrix $\mathbf{G}$, i.e.

$$\hat{\mathbf{f}} = \mathbf{P}_{R(\mathbf{G})}\mathbf{f} \ . \tag{12}$$

In Appendix A, the P optimal min/max filters are shown to be any set of filters that, with the recording illuminant, span the range space of the matrix $\mathbf{B}_p = [\mathbf{b}_1, \mathbf{b}_2, \ldots, \mathbf{b}_P]$, where the vectors $\mathbf{b}_i \quad i = 1, \ldots P$ are the P N-element vectors associated with the P largest singular values of the matrix $\mathbf{S} = [\gamma_1\mathbf{O}_1, \gamma_2\mathbf{O}_2, \ldots \gamma_K\mathbf{O}_K]$.

B. Approaches Using Information About Reflectance and Illuminant Spectra

In this section, methods of selecting color filter spaces that make use of information about the reflectance spectra in the original image are introduced. The first method uses a mean square error cost function in a normalized tristimulus space. An analytical solution for the optimal filters is obtained. The second method uses numerical methods to minimize a cost function in a perceptual color space.

1) Mean Square Error in Normalized Tristimulus Space: The cost function to be minimized is the sum of the mean square errors occurring in each of the HVISS's and can be written as

$$\epsilon_m = \sum_{i=1}^{K} \gamma_i^2 E\{\|\mathbf{O}_i^T\mathbf{f} - \mathbf{O}_i^T\hat{\mathbf{f}}\|^2\} \tag{13}$$

where the $N \times 3$-dimensional matrices $\mathbf{O}_i \quad i = 1 \ldots K$ and γ_i^2 are as defined in Section III-A.

Since statistical information about the reflectance spectra is available, the estimate $\hat{\mathbf{f}}$ is a LMMSE estimate, in which case

$$\hat{\mathbf{f}} = \mathbf{K}_f\mathbf{L}_r\mathbf{N}[\mathbf{N}^T\mathbf{L}_r\mathbf{K}_f\mathbf{L}_r\mathbf{N} + \mathbf{K}_u]^{-1}[\mathbf{c} - \bar{\mathbf{u}} - \mathbf{N}^T\mathbf{L}_r\bar{\mathbf{f}}] + \bar{\mathbf{f}} \tag{14}$$

where $\mathbf{K}_f$ is the covariance matrix of the reflectance spectra.

From the results in Appendix B, the set of P optimal filters in the absence of noise consist of any set of filters that, when combined with the recording illuminant, span the same space as the matrix $\mathbf{U}_p = [\mathbf{u}_1, \mathbf{u}_2, \ldots, \mathbf{u}_P]$, where the vectors $\mathbf{u}_i \quad i = 1, \ldots P$ are the P N-element vectors associated with the P largest eigenvalues of the matrix $\mathbf{S}\mathbf{S}^T\mathbf{K}_f$. As in Section III-A, $\mathbf{S} = [\gamma_1\mathbf{O}_1, \gamma_2\mathbf{O}_2, \ldots \gamma_K\mathbf{O}_K]$.

2)Approaches Using a Perceptual Color Error: As previously discussed, it may be more appropriate to select the filters such that a perceptual measure of color difference is minimized. If the transformation from the CIE XYZ tristimulus space to a perceptual color space is denoted by the function $\mathcal{F}[\cdot]$, then the problem can be formulated as follows: Find the filters $\mathbf{G}$ and the affine transformations defined by $\mathbf{W}_i, \mathbf{z}_i$ $i = i, \ldots K$ such that one of the following cost functions is minimized:

$$\epsilon_{\text{pmse}} = \sum_{i=1}^{K} \gamma_i^2 E\{\|\mathcal{F}[\mathbf{A}^T\mathbf{L}_{v_i}\mathbf{f}] - \mathcal{F}[\mathbf{W}_i\mathbf{G}^T\mathbf{f} + \mathbf{z}_i]\|\} \tag{15}$$

$$\epsilon_{\text{pmax1}} = \sum_{i=1}^{K} \gamma_i^2 \max_{\mathbf{f} \in R} \|\mathcal{F}[\mathbf{A}^T\mathbf{L}_{v_i}\mathbf{f}] - \mathcal{F}[\mathbf{W}_i\mathbf{G}^T\mathbf{f} + \mathbf{z}_i]\| \tag{16}$$

$$\epsilon_{\text{pmax2}} = \max_{\substack{\mathbf{f}\in R \\ i=1, \ldots K}} \gamma_i^2 \|\mathcal{F}[\mathbf{A}^T\mathbf{L}_{v_i}\mathbf{f}] - \mathcal{F}[\mathbf{W}_i\mathbf{G}^T\mathbf{f} + \mathbf{z}_i]\| \tag{17}$$

where again $\mathbf{G}^T\mathbf{f}$ denotes the recorded data, R denotes the ensemble of reflectance spectra from which the original image is derived, and $\|\cdot\|$ denotes a measure of color difference in the perceptual color space.

Transformations from the CIE XYZ color space to proposed perceptually uniform color spaces are nonlinear. The nonlinearity makes it difficult to derive an analytical solution to the above minimization problems. The CIE 1976 $L^*a^*b^*$ color space is an approximately uniform color space (see p. 166 of [35]). The transformation from CIE XYZ to $L^*a^*b^*$ is

$$\mathcal{F}(\mathbf{t}) = \mathbf{X}[t_1^{\frac{1}{3}}, t_2^{\frac{1}{3}}, t_3^{\frac{1}{3}}]^T - [16, 0, 0]^T \tag{18}$$

where

$$\mathbf{X} = \begin{bmatrix} 0 & \frac{116}{Y_n^{1/3}} & 0 \\ \frac{500}{X_n^{1/3}} & -\frac{500}{Y_n^{1/3}} & 0 \\ 0 & \frac{200}{Y_n^{1/3}} & -\frac{200}{Z_n^{1/3}} \end{bmatrix} \tag{19}$$

where $[X_n, Y_n, Z_n]$ are the CIE tristimulus values of the reference reflectance under the reference illuminant, and $\mathbf{t} = [t_1, t_2, t_3]^T$ is a CIE XYZ tristimulus value. The above transformation is used for tristimulus values satisfying the constraint $[\frac{t_1}{X_n}, \frac{t_2}{Y_n}, \frac{t_3}{Z_n}] \geq [0.008856,\ 0.008856,\ 0.008856]$. A minor modification is necessary for those tristimulus values that do not satisfy this constraint (see p. 167 of [35]). In the $L^*a^*b^*$ color space, the color difference measure between two colors is their Euclidean distance. This color difference measure is referred to as a $\Delta E_{L^*a^*b^*}$ value.

Minimization of (15), (16), or (17) can be performed using a standard unconstrained numerical optimization method [17], [8]. Depending on the transformation to the perceptual color space, it may be difficult to calculated the gradient directly, and it may be necessary to use a finite difference approximation.

IV. Physical Constraints and Sensitivity

The previous section introduced methods to specify filter spaces for obtaining colorimetric information about a scene under a number of viewing illuminants. A method of spanning the filter subspace with a set of physical filters is beyond the planned scope of this paper. A method to produce such filters is presented in [31]. However, it is of interest to verify that a realizable set exists.

Clearly, if the space to be spanned cannot be spanned by a set of nonnegative vectors, then the space cannot be spanned by a set of realizable filters. A sufficient condition for the existence of a set of nonnegative vectors that span a particular subspace is the existence of a single all positive vector in the subspace. Therefore, if an all-positive vector is found to lie in the desired filter subspace, then that filter subspace can be spanned by a set of nonnegative vectors. Two different methods of finding nonnegative filters will be discussed. A method of selecting a set of nonnegative filters with minimum sensitivity to errors in the color filters is also presented.

A. Set Theoretic Approach

Finding a set of nonnegative vectors that span a particular space is easily formulated using a set theoretic approach. If there are P filters, then the problem is to find P linearly independent vectors in the intersection of the following sets:

$$C_n = \{\ \mathbf{x}\ \mid\ x_i \geq 0\ \} \tag{20}$$

which is the set of nonnegative vectors, and

$$C_G = \{\ \mathbf{x}\ \mid \exists \mathbf{y} \quad \text{such that } \mathbf{x} = \mathbf{G}\mathbf{y}\ \} \tag{21}$$

which is the set of vectors in the range space of matrix $\mathbf{G}_{N \times P}$, where the range space of $\mathbf{G}$ defines the optimal filter subspace.

Projection onto convex sets (POCS) is an iterative method of finding an element of the intersection of a number of closed convex sets [3]. The sets C_n and C_G are both closed and convex. The intersection of the sets is also nonempty since the null vector is contained in both. The point of convergence is dependent upon the order of the projections and the initial value. To find P linearly independent vectors that lie in the intersection, it is intuitive to perform the sequential projection algorithm with P different initial conditions. If the P solution vectors are not linearly independent, then it is necessary to try additional initial conditions.

B. Linear Programming Approach

Linear programming can also be used to find vectors in the intersection of the sets C_n and C_G. The problem is to find a vector $\mathbf{n} \geq \mathbf{0}$ such that

$$\mathbf{G}\mathbf{p} = \mathbf{n} \tag{22}$$

where the vector $\mathbf{p}$ is unconstrained. An equivalent problem is to find a vector $\mathbf{n} \geq \mathbf{0}$ such that

$$\mathbf{Q}^T\mathbf{n} = \mathbf{0} \tag{23}$$

where $N(\mathbf{Q}^T) = R(\mathbf{G})^{\perp}$, and $R(\mathbf{G})^{\perp}$ denotes the orthogonal complement of $R(\mathbf{G})$. If the constraint $\sum_{i=1}^{N} n_i = 1$, where $\mathbf{n} = [n_1, \dots\ n_N]^T$ is included, then the problem becomes finding a vector $\mathbf{n} \geq \mathbf{0}$ such that

$$\begin{bmatrix} \mathbf{Q}^T \\ \mathbf{1}^T \end{bmatrix} \mathbf{n} = \begin{bmatrix} 0 \\ 1 \end{bmatrix} \tag{24}$$

where $\mathbf{1}$ is a N-dimensional vector whose elements are one, and $\mathbf{0}$ is a $N-P$-dimensional vector whose elements are zero.

Phase one of the simplex method can be used to find a basic feasible solution to the above problem and will indicate if no solution exists [17]. Once a basic feasible solution is found, additional basic feasible solutions can be found by pivoting on selected elements in the system of equations. Each basic feasible solution is a generating vector for the cone defining the intersection of the positive orthant and the range space of the matrix $\mathbf{G}$.

C. Filter Sensitivity

There are limitations to the degree of accuracy with which color filters can be fabricated. It is therefore necessary to consider the sensitivity of the color correction results to errors in the color filters. From Appendix B, an optimal set of filters can also be denoted as any matrix $\mathbf{G}$ in the set

$$C_{\mathbf{G}^*} = \{\mathbf{G} \mid \mathbf{G} = \mathbf{K}_{\mathbf{f}}^{-\frac{1}{2}}\mathbf{V}\mathbf{Y} \quad \mathbf{Y} \in M_p\} \tag{25}$$

where the columns of matrix $\mathbf{V}$ are the P eigenvectors associated with the P largest eigenvalues of the matrix $\mathbf{K}_f^{\frac{1}{2}}\mathbf{S}\mathbf{S}^T\mathbf{K}_f^{\frac{1}{2}}$, and M_p denotes the set of $P \times P$ nonsingular matrices. In Appendix C, it is shown that to reduce sensitivity of the color correction results to errors in the filters, the term $\hat{\kappa} = \frac{\sigma_{\max}}{\sigma_{\min}}$, where $\sigma_{\max}$, $\sigma_{\min}$ are the maximum and minimum singular values of the matrix $\mathbf{G}$, should be minimized. The optimization problem of finding a set of nonnegative filters that minimizes $\hat{\kappa}$ and is contained in the set $C_{\mathbf{G}^*}$ can be formulated as follows:

$$\text{Minimize } \hat{\kappa}$$

with respect to the matrix $\mathbf{Y}$, subject to

$$\mathbf{G} = \mathbf{K}_f^{-\frac{1}{2}}\mathbf{V}\mathbf{Y} \geq \mathbf{0}$$

This problem can be approached using standard constrained optimization methods [17].

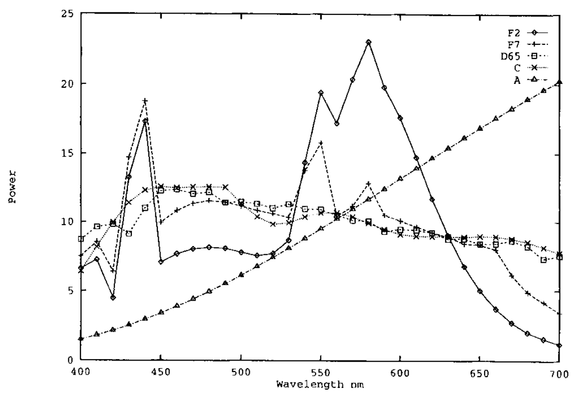

Fig. 2. Illuminants.

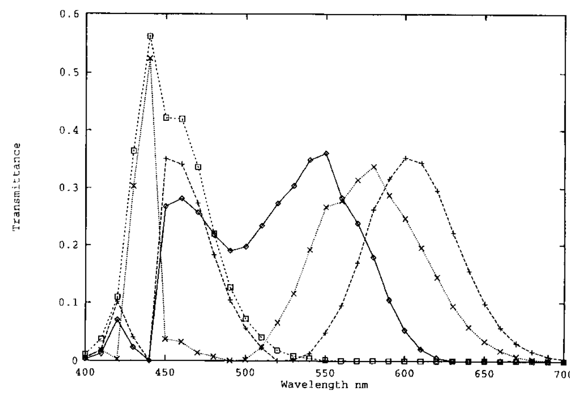

Fig. 4. Optimal four filters using only illuminant information.

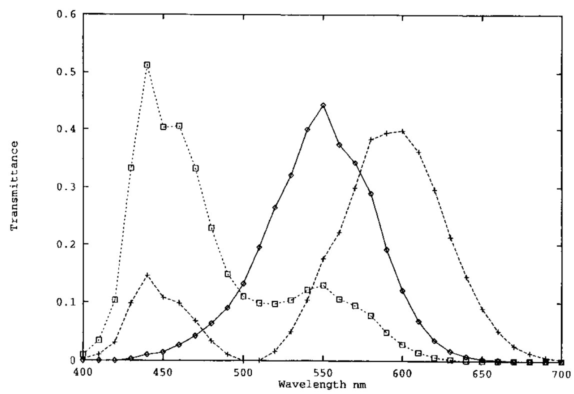

Fig. 3. Optimal three filters using only illuminant information.

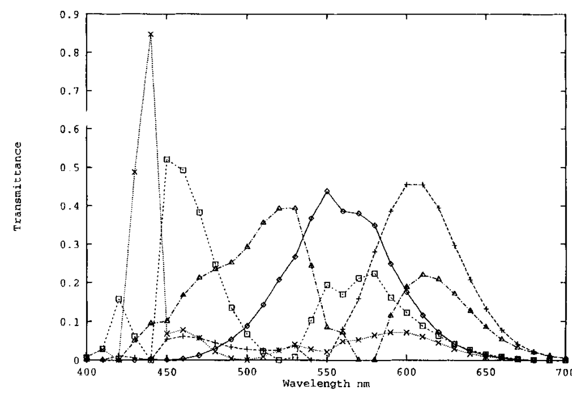

Fig. 5. Optimal five filters using only illuminant information.

V. Experiments and Results

To test the performance of the filters, experiments were performed in which the tristimulus values of reflectances under several viewing illuminants were estimated from simulated recorded data obtained from a single set of filters. Sets of color filters were calculated using information about the viewing illuminants and the HVSS. Sets of three, four, five, six, and seven optimal filters (P = 3, 4, 5, 6, 7) were derived using the method described in Section III-A for the five viewing illuminants: CIE incandescent illuminant A, CIE daylight illuminant D65, CIE fluorescent illuminant F2, CIE daylight simulation illuminant C, and CIE fluorescent illuminant F7. The viewing illuminants are shown in Fig. 2. Since there were five viewing illuminants, $K = 5$ in (9). Uniform weighting of the errors under each viewing illuminant was used so that $\gamma_i^2 = 1, \quad i = 1, \dots K$ in (9). A positive vector is contained in the subspaces defined by the filter sets; therefore, in each case, the filter subspace can be spanned by a set of nonnegative filters. The optimization problem discussed in Section IV-C was solved for each filter set using a numerical algorithms group (NAG) constrained optimization routine on a CRAY Y-MP. The optimal set of three, four, and five filters are shown in Figs. 3–5. As the number of filters increases to six and seven, multiple sharp peaks occur in the filter transmittances.

To measure the performance of the filter sets, errors were computed over ensembles of recorded reflectance spectra. A spectral sampling width of 10 nm was used, which resulted in $N = 31$ samples between 400 and 700 nm. The first data set consisted of 343 spectral reflectances produced from a Cannon color copier. The second data set consisted of 512 spectral reflectances produced from a Kodak thermal dye transfer printer. The third data set consisted of 64 spectral reflectances recorded from a selection of Munsell chips. The copier and thermal data sets were produced from varying densities of cyan, magenta, and yellow colorants. The Munsell data set was produced by pigments.

Sets of color filters were calculated using information about the viewing illuminants and statistics about the reflectances to be recorded. Sets of three, four, and five optimal filters ($P = 3, 4, 5$) were derived using the method described in Section III-B for each of the data sets with the five illuminants A, D65, F2, C, and F7. Uniform weighting of the errors under each viewing illuminant was used so that $\gamma_i^2 = 1 \quad i = 1, \dots K$ in (13). For each set of filters, one filter was positive; therefore, the space in each case can be spanned by a set of nonnegative filters. Again, the optimization problem discussed in Section IV-C was solved for each filter set using a NAG constrained optimization routine on a CRAY Y-MP. The optimal set of

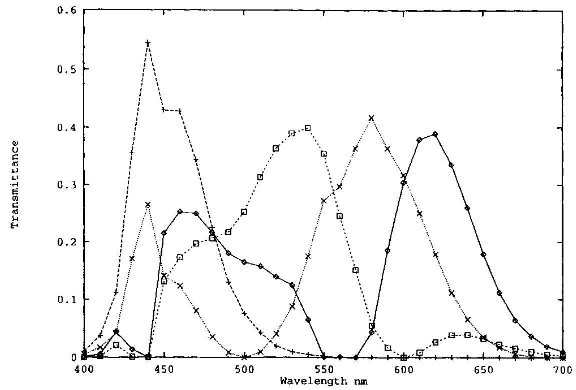

Fig. 6. Optimal four filters for copier data set.

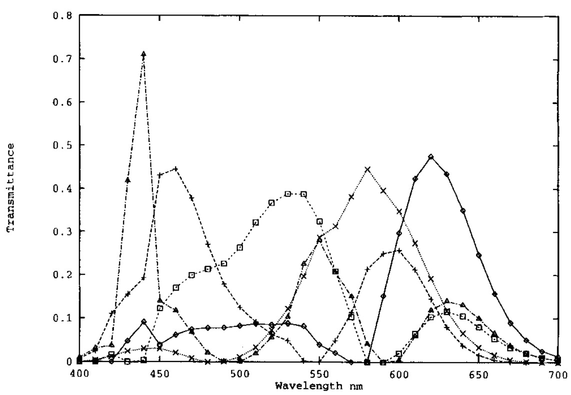

Fig. 7. Optimal five filters for copier data set.

four and five filters for the copier data set are shown in Figs. 6 and 7. The optimal three filters for the copier data set vary only slightly from that shown in Fig. 3.

A simulation was performed in which the P-stimulus values of the reflectance spectra were obtained using each of the derived filter sets. The recorded data using the filter set $\mathbf{G}$ is

$$\mathbf{c}_j = \mathbf{G}^T\mathbf{f}_j \quad j = 1, 2 \cdots N_f. \tag{26}$$

where N_f is the number of reflectance spectra in the particular ensemble. The CIE tristimulus values for each reflectance ensemble were calculated using each of the five viewing illuminants. This can be written as

$$\mathbf{t}_{ij} = \mathbf{A}^T\mathbf{L}_{v_i}\mathbf{f}_j \quad j = 1, 2 \ldots N_f \quad i = 1, 2, \ldots 5. \tag{27}$$

For the filters that used information only about the viewing illuminants, the estimated CIE tristimulus values were calculated using a minimum norm ML estimator. The estimate $\hat{\mathbf{t}}_{ij}$ is

$$\hat{\mathbf{t}}_{ij} = \mathbf{A}^T\mathbf{L}_{v_i}(\mathbf{G}^T)^{\dagger}\mathbf{c}_j \ . \tag{28}$$

For the filters that used information about the reflectance spectra, the CIE tristimulus values were estimated from the recorded data using a LMMSE estimator. The estimate $\hat{\mathbf{t}}_{ij}$ is

$$\hat{\mathbf{t}}_{ij} = \mathbf{A}^T\mathbf{L}_{v_i}\mathbf{K}_f\mathbf{G}[\mathbf{G}^T\mathbf{K}_f\mathbf{G}]^{-1}[\mathbf{c}_j - \mathbf{G}^T\bar{\mathbf{f}}] + \mathbf{A}^T\mathbf{L}_{v_i}\bar{\mathbf{f}}. \tag{29}$$

TABLE I

$\Delta E_{L^*a^*b^*}$ VALUES FOR COLOR CORRECTIONS USING THE COPIER DATA SET WITH COPIER COVARIANCE AND MEAN IN THE LMMSE ESTIMATOR

Illum	Errors	HVSS	3 Filters Copier Set	4 Filters Copier Set	5 Filters Copier Set
A	ΔE_{avg}	3.24	2.76	0.50	0.17
	$\Delta E_{\max}$	14.16	11.00	2.39	1.47
	$\Delta E \geq 3$	145	121	0	0
D65	ΔE_{avg}	0.75	1.43	0.31	0.27
	$\Delta E_{\max}$	2.80	6.92	1.05	1.19
	$\Delta E \geq 3$	0	36	0	0
F2	ΔE_{avg}	3.08	2.16	0.95	0.61
	$\Delta E_{\max}$	23.48	14.94	3.48	2.98
	$\Delta E \geq 3$	110	65	5	0
C	ΔE_{avg}	0.53	1.23	0.21	0.16
	$\Delta E_{\max}$	1.94	6.35	0.74	0.70
	$\Delta E \geq 3$	0	26	0	0
F7	ΔE_{avg}	0.75	1.24	0.21	0.11
	$\Delta E_{\max}$	2.62	4.89	1.35	0.93
	$\Delta E \geq 3$	0	21	0	0
	MSE	1.53E-3	1.30E-3	1.55E-4	3.83E-5

In practice, although a set of optimal filters is derived using information about a particular spectral reflectance ensemble, the filter set may actually be used on a wide range of images. If the covariance matrix and mean are unknown for the reflectance spectra being recorded, then the covariance and mean for the reflectance spectra from which the filters were derived could be used in the LMMSE estimator. If the covariance matrix and mean of the reflectance spectra are known, then that information could be used in the LMMSE estimator even though the filters were not optimal for that data set. In either situation, the mean square error will be larger than if optimal filters for the data set being recorded were used along with the correct statistics in the LMMSE estimator.

The $\Delta E_{L^*a^*b^*}$ values between $\hat{\mathbf{t}}_{ij}$ and $\mathbf{t}_{ij}$ were calculated for several different cases and are contained in Tables I–XII. The average color tolerance accepted in printing applications has been studied and found to be approximately a $\Delta E_{L^*a^*b^*}$ of six [25]. The standard deviation in the accepted tolerance was 3.63 $\Delta E_{L^*a^*b^*}$. In another study, the perceptibility tolerance for pictorial images was investigated and the average $\Delta E_{L^*a^*b^*}$ was found to be 2.15 [27]. If the $\Delta E_{L^*a^*b^*}$ value between two colors is less than three, then the colors are difficult to visually distinguish. The values in the tables are denoted as follows:

- ΔE_{avg} average $\Delta E_{L^*a^*b^*}$ value of the set
- $\Delta E_{\max}$ maximum $\Delta E_{L^*a^*b^*}$ in the set
- $\Delta E \geq 3$ number of errors with a $\Delta E_{L^*a^*b^*}$ greater than three
- MSE sum of the mean square errors defined by (13).

For a particular viewing illuminant, the white point of a data set was the CIE tristimulus value of the data set's reference white spectral reflectance under the viewing illuminant. The

TABLE II

$\Delta E_{L^*a^*b^*}$ VALUES FOR COLOR CORRECTIONS USING THE THERMAL DATA SET WITH THERMAL COVARIANCE AND MEAN IN THE LMMSE ESTIMATOR

Illum	Errors	HVSS	3 Filter Thermal set	4 Filters Thermal set	5 Filters Thermal set
A	ΔE_{avg}	4.29	3.83	1.40	0.38
	ΔE_{max}	21.41	15.34	8.00	4.14
	$\Delta E \geq 3$	270	265	65	3
D65	ΔE_{avg}	1.30	1.54	0.66	0.54
	ΔE_{max}	6.81	6.59	3.10	3.18
	$\Delta E \geq 3$	38	65	2	2
F2	ΔE_{avg}	3.48	2.98	1.94	1.11
	ΔE_{max}	23.81	15.09	7.86	7.67
	$\Delta E \geq 3$	229	197	99	28
C	ΔE_{avg}	0.86	1.28	0.52	0.37
	ΔE_{max}	4.79	6.09	1.81	2.24
	$\Delta E \geq 3$	18	40	0	0
F7	ΔE_{avg}	1.08	1.68	0.69	0.28
	ΔE_{max}	3.72	8.81	3.76	2.44
	$\Delta E \geq 3$	2	62	12	0
	MSE	2.47E-3	2.14E-3	3.36E-4	8.65E-5

TABLE III

$\Delta E_{L^*a^*b^*}$ VALUES FOR COLOR CORRECTIONS USING THE MUNSELL DATA SET WITH MUNSELL COVARIANCE AND MEAN IN THE LMMSE ESTIMATOR

Illum	Errors	HVSS	3 Filters Munsell Set	4 Filters Munsell Set	5 Filters Munsell Set
A	ΔE_{avg}	2.71	2.31	0.71	0.30
	ΔE_{max}	8.95	7.91	2.82	1.52
	$\Delta E \geq 3$	21	15	0	0
D65	ΔE_{avg}	0.72	1.24	0.38	0.25
	ΔE_{max}	2.40	4.59	1.68	1.04
	$\Delta E \geq 3$	0	3	0	0
F2	ΔE_{avg}	2.17	1.52	1.08	0.62
	ΔE_{max}	9.41	6.36	3.83	2.40
	$\Delta E \geq 3$	14	5	4	0
C	ΔE_{avg}	0.47	1.07	0.43	0.15
	ΔE_{max}	1.62	3.72	1.58	0.80
	$\Delta E \geq 3$	0	4	0	0
F7	ΔE_{avg}	0.79	1.26	0.34	0.21
	ΔE_{max}	2.44	4.29	1.21	0.80
	$\Delta E \geq 3$	0	5	0	0
	MSE	4.18E-3	3.50E-3	6.93E-4	8.00E-5

reference white spectral reflectance of the copier data set was the spectral reflectance of the paper from which the data set was measured. The reference white spectral reflectance of the thermal data set was also that of the paper from which the data set was measured. The reference white spectral reflectance for the Munsell data set was that of a spectrally uniform reflectance.

In the tables, the filters labeled HVSS refer to a set of filters that, with a uniform recording illuminant, spanned the HVSS. One such set would be the CIE color matching functions shown in Fig. 1. This set of filters was used as a benchmark since, in the design of commercial desktop scanners, attempts are often made to span the HVSS. In Tables I–IX, the filters labeled 3, 4, or 5 filters Copier set; 3, 4, or 5 filters Thermal set; and 3, 4, or 5 filters Munsell set refer to filters derived using statistical information about the copier data set, thermal data set, and Munsell data set, respectively. In Tables X–XII, The filters labeled 3, 4, 5, 6, or 7 filters illum. refer to the filters derived using only information about the viewing illuminants. In Table XV, the columns labeled ϵ_{pmse}, ϵ_{pmax1}, ϵ_{pmax2}, and LMMSE indicate that the results were obtained using the filters and transformations from (15)–(17) and Section III-B-1, respectively.

A. Discussion of Results

Most color imaging devices currently use three-color filters to achieve color separation. The results of this work indicate that a significant improvement in color correction results is possible with the addition of a fourth filter. Although an improvement is certainly expected, the magnitude of the improvement with the additional filter is surprising. Tables I–III contain the $\Delta E_{L^*a^*b^*}$ values for the copier data set, thermal data set, and Munsell data set, respectively, using the statistics in the LMMSE estimator and the optimal filters associated with the recorded data set. The optimal four filters in Tables I–III reduced the $\Delta E_{L^*a^*b^*}$ values significantly, especially the maximum errors. In several cases, the maximum error is reduced from one that would be visually noticeable to one that would not be visually perceived. The addition of a fifth filter did not provide a large improvement over the four-filter case when using a LMMSE estimator for these data sets. In one case (Table II, illuminant C, 5 filters), the addition of a fifth filter resulted in an increase in the maximum $\Delta E_{L^*a^*b^*}$ error. This can be explained by the fact that the cost function is MSE not ΔE_{max}. It is noted that for illuminants D65, C, and F7, the HVSS filters perform better than the optimal three filters. For illuminants A and F2, the HVSS filters produce significant color errors. The advantage of using an optimal set of three filters over the HVSS filters is discussed in Section V-B.

Tables IV–VI display the results of using filters derived from one ensemble of spectral reflectances on a different ensemble of spectral reflectances. This was performed to investigate the sensitivity of the results to variations in the filters. The statistics corresponding to the data set being recorded are used in the LMMSE estimator. Again, using four filters produced a significant drop in the $\Delta E_{L^*a^*b^*}$ values, and the addition of a fifth filter did not provide a significant improvement over the four filter case. In four cases, the addition of a fifth filter resulted in a slight increase in the maximum $\Delta E_{L^*a^*b^*}$ error (e.g., Table V, illuminant F2, 5 filters Munsell). This can be explained by the fact that suboptimal filters are used and that ΔE_{max} is not the cost function. Comparison of Tables I–III with Tables IV–VI give some indication of the sensitivity of

TABLE IV
COMPARISON OF THE $\Delta E_{L^*a^*b^*}$ VALUES FOR THE COPIER ENSEMBLE USING VARIOUS FILTER SETS AND USING THE COPIER STATISTICS IN THE LMMSE ESTIMATORS

Illum	Errors	3 Filters Munsell Set	3 Filters Thermal Set	4 Filters Munsell Set	4 Filters Thermal Set	5 Filters Munsell Set	5 Filters Thermal Set
A	ΔE_{avg}	2.72	2.73	0.50	0.50	0.27	0.18
	ΔE_{max}	11.00	10.94	2.57	2.53	2.06	1.43
	$\Delta E \geq 3$	118	118	0	0	0	0
D65	ΔE_{avg}	1.54	1.50	0.32	0.34	0.29	0.32
	ΔE_{max}	7.41	7.20	1.19	1.18	1.12	1.33
	$\Delta E \geq 3$	41	39	0	0	0	0
F2	ΔE_{avg}	2.06	2.11	0.93	0.95	0.66	0.66
	ΔE_{max}	14.09	14.48	3.55	3.52	3.18	3.08
	$\Delta E \geq 3$	60	61	5	5	1	1
C	ΔE_{avg}	1.34	1.30	0.29	0.28	0.13	0.20
	ΔE_{max}	6.87	6.66	1.08	1.08	0.53	0.80
	$\Delta E \geq 3$	29	28	0	0	0	0
F7	ΔE_{avg}	1.34	1.30	0.25	0.23	0.15	0.11
	ΔE_{max}	5.29	5.14	1.57	1.50	1.11	0.85
	$\Delta E \geq 3$	28	23	0	0	0	0
	MSE	1.30E-3	1.30E-3	1.65E-4	1.64E-4	4.31E-5	4.02E-5

TABLE V
COMPARISON OF THE $\Delta E_{L^*a^*b^*}$ VALUES FOR THE THERMAL ENSEMBLE USING VARIOUS FILTER SETS AND USING THE THERMAL STATISTICS IN THE LMMSE ESTIMATOR

Illum	Errors	3 Filters Copier Set	3 Filters Munsell Set	4 Filters Copier Set	4 Filters Munsell Set	5 Filters Copier Set	5 Filters Munsell Set
A	ΔE_{avg}	3.89	3.80	1.36	1.40	0.39	0.60
	ΔE_{max}	15.61	14.66	7.03	8.06	4.44	6.42
	$\Delta E \geq 3$	267	265	58	65	4	16
D65	ΔE_{avg}	1.46	1.59	0.62	0.64	0.49	0.53
	ΔE_{max}	6.29	6.80	3.17	2.84	2.76	3.18
	$\Delta E \geq 3$	54	68	2	0	0	2
F2	ΔE_{avg}	3.01	2.96	1.97	1.93	1.09	1.22
	ΔE_{max}	15.59	14.68	8.07	7.73	7.77	8.97
	$\Delta E \geq 3$	202	196	102	98	28	39
C	ΔE_{avg}	1.19	1.34	0.44	0.52	0.33	0.30
	ΔE_{max}	5.79	6.33	1.45	1.86	1.92	1.82
	$\Delta E \geq 3$	33	49	0	0	0	0
F7	ΔE_{avg}	1.60	1.73	0.61	0.72	0.29	0.39
	ΔE_{max}	8.30	9.39	3.22	3.88	2.76	3.55
	$\Delta E \geq 3$	56	69	7	14	0	2
	MSE	2.14E-3	2.14E-3	3.56E-4	3.37E-4	9.10E-5	9.42E-5

TABLE VI
COMPARISON OF THE $\Delta E_{L^*a^*b^*}$ VALUES FOR THE MUNSELL ENSEMBLE USING VARIOUS FILTER SETS AND USING THE MUNSELL STATISTICS IN THE LMMSE ESTIMATOR

Illum	Errors Set	3 Filters Copier Set	3 Filters Thermal Set	4 Filters Copier Set	4 Filters Thermal Set	5 Filters Copier Set	5 Filters Thermal Set
A	ΔE_{avg}	2.37	2.33	0.75	0.72	0.21	0.22
	ΔE_{max}	8.00	7.92	2.72	2.87	1.21	1.12
	$\Delta E \geq 3$	15	15	0	0	0	0
D65	ΔE_{avg}	1.13	1.20	0.31	0.38	0.27	0.30
	ΔE_{max}	4.31	4.50	1.21	1.67	1.14	1.33
	$\Delta E \geq 3$	3	3	0	0	0	0
F2	ΔE_{avg}	1.59	1.56	1.15	1.09	0.62	0.63
	ΔE_{max}	6.78	6.49	4.17	3.87	2.59	2.58
	$\Delta E \geq 3$	6	5	0	0	0	0
C	ΔE_{avg}	0.96	1.03	0.33	0.42	0.19	0.21
	ΔE_{max}	3.44	3.63	1.30	1.57	0.99	1.13
	$\Delta E \geq 3$	1	2	0	0	0	0
F7	ΔE_{avg}	1.15	1.22	0.27	0.33	0.19	0.18
	ΔE_{max}	3.70	4.08	0.95	1.22	0.64	0.64
	$\Delta E \geq 3$	4	5	0	0	0	0
	MSE	3.51E-3	3.50E-3	7.46E-4	6.94E-4	9.26E-5	8.88E-5

TABLE VII
COMPARISON OF THE $\Delta E_{L^*a^*b^*}$ VALUES FOR THE COPIER ENSEMBLE USING VARIOUS FILTER SETS WITH THE STATISTICS IN THE LMMSE ESTIMATOR CORRESPONDING TO THE FILTER SET USED TO RECORD THE DATA

Illum	Errors	3 Dilters Munsell Set	3 Filters Thermal Set	4 Filters Munsell Set	4 Filters Thermal Set	5 Filters Munsell Set	5 Filters Thermal Set
A	ΔE_{avg}	4.08	5.94	0.77	1.71	0.44	0.35
	ΔE_{max}	18.09	25.92	1.75	4.16	2.03	1.32
	$\Delta E \geq 3$	171	249	0	28	0	0
D65	ΔE_{avg}	2.33	2.10	0.93	0.85	0.43	0.72
	ΔE_{max}	7.94	5.41	3.04	2.33	1.76	2.37
	$\Delta E \geq 3$	101	73	1	0	0	0
F2	ΔE_{avg}	2.74	2.58	2.24	2.89	1.00	1.47
	ΔE_{max}	16.36	8.29	7.55	6.26	4.22	5.21
	$\Delta E \geq 3$	106	107	69	165	10	33
C	ΔE_{avg}	2.10	2.11	0.97	0.89	0.19	0.45
	ΔE_{max}	7.18	5.00	2.93	2.42	0.82	1.75
	$\Delta E \geq 3$	83	70	0	0	0	0
F7	ΔE_{avg}	1.94	2.70	0.38	0.83	0.31	0.27
	ΔE_{max}	5.88	7.35	1.20	1.80	1.43	1.30
	$\Delta E \geq 3$	76	127	0	0	0	0
	MSE	3.68E-3	5.06E-3	7.41E-4	1.22E-3	1.22E-4	1.68E-4

the results to variations in the filter spectral responses. The errors obtained indicate that using filters that were optimal for one data set work well with other data sets, given that the proper statistics are used in the LMMSE estimators.

Tables VII–IX display the results of using statistics in the LMMSE estimator, which correspond to the filters set used to record the data. Since suboptimal filters are used along with incorrect statistics in the LMMSE estimators, the results should be worse than those obtained in Tables I–VI. The improvement with the addition of a fourth filter is again noticeable. Using incorrect statistics in the LMMSE estimators and suboptimal filters, the average $\Delta E_{L^*a^*b^*}$ value increased slightly, with the addition of a filter, for six cases. Except for

TABLE VIII
COMPARISON OF THE $\Delta E_{L^*a^*b^*}$ VALUES FOR THE THERMAL ENSEMBLE USING VARIOUS FILTER SETS WITH THE STATISTICS IN THE LMMSE ESTIMATOR CORRESPONDING TO THE FILTER SET USED TO RECORD THE DATA

Illum	Errors	3 Filters Copier Set	3 Filters Munsell Set	4 Filters Copier Set	4 Filters Munsell Set	5 Filters Copier Set	5 Filters Munsell Set
	ΔE_{avg}	6.96	5.20	1.51	1.58	0.68	1.16
A	$\Delta E_{\max}$	22.67	18.64	10.01	6.31	9.21	3.36
	$\Delta E \geq 3$	416	336	59	50	18	2
	ΔE_{avg}	2.97	2.18	0.93	1.00	0.91	1.21
D65	$\Delta E_{\max}$	14.43	11.28	3.08	2.43	5.96	3.61
	$\Delta E \geq 3$	197	127	2	0	16	14
	ΔE_{avg}	4.34	4.01	2.57	2.77	2.01	2.79
F2	$\Delta E_{\max}$	25.51	29.97	10.27	6.32	15.48	7.05
	$\Delta E \geq 3$	264	296	156	233	83	241
	ΔE_{avg}	2.88	2.00	0.61	0.68	0.64	0.70
C	$\Delta E_{\max}$	13.09	10.76	2.85	2.42	2.87	1.92
	$\Delta E \geq 3$	197	112	0	0	0	0
	ΔE_{avg}	3.62	2.81	0.64	0.79	0.48	0.66
F7	$\Delta E_{\max}$	12.83	8.66	3.62	2.81	5.99	1.87
	$\Delta E \geq 3$	281	191	5	0	11	0
	MSE	5.92E-3	3.75E-3	9.37E-4	8.57E-4	2.80E-4	4.27E-4

one case, this increase occurred when going from four to five filters (see Table VII, illuminant F2, 4 filters Thermal for the exception). The effect of an increase in average $\Delta E_{L^*a^*b^*}$ can be accounted for by the fact that incorrect statistics and suboptimal filters were used and that a MSE cost function was used.

Tables X–XII contain $\Delta E_{L^*a^*b^*}$ values for the data sets using filters obtained using only illuminant information and a minimum norm ML estimator. This is equivalent to assuming zero mean, uncorrelated spectra in the LMMSE estimator, which is not a good assumption. The lack of information about the reflectance spectra resulted in larger errors, as should be expected. Note that in several cases an increase in the number of filters resulted in an increase in the average $\Delta E_{L^*a^*b^*}$ values and maximum $\Delta E_{L^*a^*b^*}$ values for the set. This increase is accounted for by the fact that the cost function that was minimized was the maximum square error and not the average or maximum $\Delta E_{L^*a^*b^*}$ values.

B. Illuminant Subspace Weighting

As noted earlier, in Tables I–III, the HVSS filters perform well for the illuminants D65, C, and F7 but perform poorly for the illuminants A and F2. The optimal three filters produce lower errors in illuminants A and F2 than the HVSS filters at the expense of larger errors in illuminants D65, C, and F7. Suppose that the goal is to obtain the smallest errors under each illuminant such that the errors under each illuminant are of the same magnitude.

The weighting factors γ_i can be used to weight the importance of color errors undervarious illuminants. A measure of how well three filters obtain colorimetric information of the scene for a particular illuminant $\mathbf{L}_{v_i}$ can aid in the selection of the γ_i to equalize the errors across the illuminants. Consider a distance measure between the range space of the filters $R(\mathbf{G})$, and the range space the filters should ideally span $R(\mathbf{L}_{v_i}\mathbf{A})$. The distance measure is

$$\theta_{G,i} = \|\mathbf{P}_G - \mathbf{P}_{L_i A}\|_2 \tag{30}$$

where $\mathbf{P}_G$, $\mathbf{P}_{L_i A}$ are the orthogonal projection operators onto $R(\mathbf{G})$ and $R(\mathbf{L}_{v_i}\mathbf{A})$, respectively, $\theta_{G,i}$ is the maximum principal angle, and the norm is the matrix spectral norm (see pp. 58, 76–78, 584–585 of [9]). This measure has been suggested in previous color work [32] and signal-processing applications [22].

The color correction errors are dependent on the reflectance spectra. The above measure does not incorporate information about the reflectance spectra that may be used in the estimation process. The distance measure between the three filters $\mathbf{G}$ and the HVISS $\mathbf{L}_{v_i}\mathbf{A}$ for reflectance spectra with covariance matrix $\mathbf{K}_f$ is defined as

$$\chi_{G,i} = \left\| \mathbf{P}_{K_f^{\frac{1}{2}} G} - \mathbf{P}_{K_f^{\frac{1}{2}} L_i A} \right\|_2 \tag{31}$$

where $\mathbf{P}_{K_f^{\frac{1}{2}} G}$, $\mathbf{P}_{K_f^{\frac{1}{2}} L_i A}$ are the orthogonal projection operators onto $R(\mathbf{K}_f^{\frac{1}{2}}\mathbf{G})$ and $R(\mathbf{K}_f^{\frac{1}{2}}\mathbf{L}_{v_i}\mathbf{A})$, respectively. If the reflectance spectra are uncorrelated (which is unlikely for natural objects), then $\mathbf{K}_f^{\frac{1}{2}} = \mathbf{I}$ and $\chi_{G,i} = \theta_{G,i}$. Alternatively, consider the case in which the reflectance spectra are highly correlated. In particular, consider the case in which the reflectance spectra are contained in a 3-D subspace. If the basis vectors, which define the reflectance subspace, are linearly independent after projection onto the filter subspace, then the reflectance spectra can be calculated exactly from the recorded data [32]. In this case, perfect color correction follows, and the value $\chi_{G,i}$ will be zero.

To check the correlation of $\chi_{G,i}$ with the color errors in Table I, $\chi_{G,i}$ was calculated for the copier data with the HVSS filters and for the copier data with the three optimal copier filters. The χ values are contained in rows one and two of Table XIII. Note that the χ values correlate well with the color correction results. The distance between the filter subspace and a HVISS is a good measure of how well the filter set obtains tristimulus values for that illuminant and explains the relative poor performance of the HVSS filters for the illuminants A and F2.

Using weights of $\gamma_i = \sqrt{\chi_{G,i}}$, in (13), where $\mathbf{G}$ is the three optimal copier filters for $\gamma_i = 1$, the errors for illuminant A and F2 should decrease at the expense of increased errors for the remaining illuminants. The resulting filter set is denoted in Table XIII as three filters Copier Weighted. From the values in Table XIII, observe that the weighted filter set is approximately an equal distance from each of the five subspaces defined by the illuminants and Munsell spectra. For direct comparison, Table XIV contains the color errors for the HVSS filters, the optimal copier filters, and the weighted copier filters. For the weighted copier filters, the color errors are approximately

TABLE IX
COMPARISON OF THE $\Delta E_{L^*a^*b^*}$ VALUES FOR THE MUNSELL ENSEMBLE USING VARIOUS FILTER SETS WITH THE STATISTICS USED IN THE LMMSE ESTIMATOR CORRESPONDING TO THE FILTER SET USED TO RECORD THE DATA

Illum	Errors	3 Filters Copier set	3 Filters Thermal set	4 Filters Copier set	4 Filters Thermal set	5 Filters Copier set	5 Filters Thermal set
	ΔE_{avg}	3.46	2.76	0.96	1.30	0.46	0.45
A	$\Delta E_{\max}$	9.97	11.49	4.30	6.79	4.26	2.32
	$\Delta E \geq 3$	35	21	6	0	2	0
	ΔE_{avg}	1.99	1.22	0.50	0.70	0.52	0.67
D65	$\Delta E_{\max}$	6.33	3.79	2.09	2.18	3.32	2.37
	$\Delta E \geq 3$	16	2	0	0	2	0
	ΔE_{avg}	2.15	2.12	1.57	1.99	1.16	1.37
F2	$\Delta E_{\max}$	6.11	5.06	6.92	5.60	8.47	4.48
	$\Delta E \geq 3$	13	14	7	12	2	5
	ΔE_{avg}	1.72	1.03	0.41	0.52	0.29	0.46
C	$\Delta E_{\max}$	5.67	3.44	2.15	1.26	1.54	1.87
	$\Delta E \geq 3$	11	3	0	0	0	0
	ΔE_{avg}	1.83	1.38	0.41	0.64	0.35	0.33
F7	$\Delta E_{\max}$	5.54	4.96	1.87	2.75	2.20	1.26
	$\Delta E \geq 3$	11	6	0	0	0	0
	MSE	$3.51\text{E}-3$	$5.23\text{E}-3$	$7.46\text{E}-4$	$1.28\text{E}-3$	$9.26\text{E}-5$	$3.56\text{E}-4$

TABLE X
$\Delta E_{L^*a^*b^*}$ VALUES FOR COLOR CORRECTIONS USING THE DATA SET AND MINIMUM NORM MAXIMUM LIKELIHOOD ESTIMATOR

Illum	Errors	HVSS	3 Filters illum	4 Filters illum	5 Filters illum	6 Filters illum	7 Filters illum
	ΔE_{avg}	12.64	12.24	8.63	2.77	0.64	0.39
A	$\Delta E_{\max}$	24.60	26.05	16.00	8.75	1.50	0.68
	$\Delta E \geq 3$	343	343	340	126	0	0
	ΔE_{avg}	3.18	5.58	6.77	1.09	0.36	0.29
D65	$\Delta E_{\max}$	5.48	10.56	15.12	3.94	0.92	0.51
	$\Delta E \geq 3$	200	329	329	17	0	0
	ΔE_{avg}	7.25	4.62	9.49	3.91	0.60	0.55
F2	$\Delta E_{\max}$	16.45	11.18	30.08	12.69	1.14	1.41
	$\Delta E \geq 3$	343	330	340	179	0	0
	ΔE_{avg}	2.54	4.97	5.20	1.12	0.37	0.29
C	$\Delta E_{\max}$	4.53	8.34	11.06	3.83	1.09	0.66
	$\Delta E \geq 3$	57	328	310	17	0	0
	ΔE_{avg}	2.98	5.81	2.71	0.72	0.64	0.66
F7	$\Delta E_{\max}$	5.06	11.46	8.75	3.35	2.62	1.99
	$\Delta E \geq 3$	171	337	108	8	0	0

TABLE XI
$\Delta E_{L^*a^*b^*}$ VALUES FOR COLOR CORRECTIONS USING THE THERMAL DATA SET AND MINIMUM NORM MAXIMUM LIKELIHOOD ESTIMATOR

Illum	Errors	HVSS	3 Filters illum	4 Filters illum	5 Filters illum	6 Filters illum	7 Filters illum
	ΔE_{avg}	6.42	6.51	5.57	2.77	0.93	0.48
A	$\Delta E_{\max}$	22.29	10.01	18.81	14.66	2.52	0.98
	$\Delta E \geq 3$	395	402	353	154	0	0
	ΔE_{avg}	2.84	3.75	4.88	1.19	0.57	0.39
$D65$	$\Delta E_{\max}$	6.36	10.25	19.19	4.96	1.82	0.94
	$\Delta E \geq 3$	153	292	352	57	0	0
	ΔE_{avg}	5.21	4.28	8.60	3.47	0.36	0.39
$F2$	$\Delta E_{\max}$	19.23	14.77	43.25	16.30	2.18	2.35
	$\Delta E \geq 3$	390	352	459	170	0	0
	ΔE_{avg}	2.17	3.07	3.65	1.22	0.39	0.30
C	$\Delta E_{\max}$	3.57	8.46	15.16	4.72	1.11	1.29
	$\Delta E \geq 3$	38	226	256	61	0	0
	ΔE_{avg}	2.08	3.42	2.64	0.85	0.65	0.62
F7	$\Delta E_{\max}$	7.60	13.25	17.72	4.32	4.50	3.38
	$\Delta E \geq 3$	123	223	133	33	22	3

uniformly distributed among the five illuminants, which was the original goal.

An advantage of this approach over using the HVSS filters is that the γ_i in (13) or (9) can be adjusted to reduce errors under one illuminant at the expense of another. Therefore, the designer can distribute the color errors under the various illuminants. In addition, the method indicates what subspace the filters should span if more than three filters can be used in the recording process.

C. Perceptual Cost Functions

As previously discussed the MSE is not the best measure of perceptual error. The cost functions (15)–(17) may be more appropriate. Minimization of the perceptual cost functions, with respect to the filters $\mathbf{G}$ and the affine transformations $\mathbf{W}_i, \mathbf{z}_i \quad i = 1, \ldots K$, can become computationally expensive due to the large number of variables involved. To test the improvement that is obtained by using the cost functions (15)–(17), sets of three optimal filters and the optimal affine transformations were calculated for the Munsell data set with the CIE illuminants A, D65, and F2. The perceptual color space was the CIE $L^*a^*b^*$ color space. The minimizations of (15)–(17) were performed on a CRAY Y-MP. For comparison, three optimal filters using the method described in Section III-B-1 were derived for the Munsell data set with the CIE illuminants A, D65, and F2. The results are contained in Table XV.

In Table XV, Illum ΔE_{avg} and Illum $\Delta E_{\max}$ denote the average of ΔE_{avg} and $\Delta E_{\max}$ over the illuminants, respectively. Cost functions (15) and (16) are used to minimize ΔE_{avg} and Illum $\Delta E_{\max}$, respectively. Cost function (17) is used to minimize $\Delta E_{\max}$ over the illuminants. Note that the HVSS filters produce the largest color errors of the five filter sets, as should be expected. The $\epsilon_{p\max 2}$ filters, which minimize $\Delta E_{\max}$ over the illuminants, produced the largest number of color errors with a total of 46. Of course, none of those color errors were greater than a $\Delta E_{L^*a^*b^*}$ of 4.05 and may be difficult to detect. Finally, note that the LMMSE filters performance is close to that of the ϵ_{pmse} filters. For this

TABLE XII
$\Delta E_{L^*a^*b^*}$ VALUES FOR COLOR CORRECTIONS USING THE MUNSELL DATA SET AND MINIMUM NORM MAXIMUM LIKELIHOOD ESTIMATOR

Illum	Errors	HVSS	3 Filters illum	4 Filters illum	5 Filters illum	6 Filters illum	7 Filters illum
	ΔE_{avg}	8.47	8.99	6.95	3.15	0.57	0.32
A	ΔE_{max}	16.55	14.95	14.53	9.81	1.40	0.63
	$\Delta E \geq 3$	63	64	61	30	0	0
	ΔE_{avg}	2.53	3.75	5.04	1.18	0.36	0.29
D65	ΔE_{max}	5.49	9.33	12.84	4.39	1.08	0.75
	$\Delta E \geq 3$	17	38	53	4	0	0
	ΔE_{avg}	4.76	3.43	7.89	4.34	0.37	0.45
F2	ΔE_{max}	14.89	10.00	26.15	14.96	1.18	1.80
	$\Delta E \geq 3$	43	33	61	37	0	0
	ΔE_{avg}	1.96	3.21	3.74	1.27	0.24	0.24
C	ΔE_{max}	3.36	7.19	9.28	4.37	0.95	0.68
	$\Delta E \geq 3$	3	32	39	4	0	0
	ΔE_{avg}	2.85	4.49	2.32	0.65	0.82	0.62
F7	ΔE_{max}	5.71	10.18	7.52	3.32	3.71	2.66
	$\Delta E \geq 3$	29	48	16	2	2	0

TABLE XIII
χ VALUES FOR FILTER SETS

filters	Illum A	Illum D65	Illum F2	Illum C	Illum F7
HVSS	0.091	0.019	0.053	0.015	0.022
Copier 3 $\gamma_i = 1$	0.075	0.033	0.038	0.029	0.032
Copier 3 Weighted	0.057	0.049	0.040	0.046	0.050

spectral reflectance data set and set of illuminants, a LMMSE cost function is not unreasonable to use for minimizing the $\Delta E_{L^*a^*b^*}$ errors.

VI. CONCLUSION

Methods were introduced for selecting a subspace an optimal set of color filters should span given only spectral information about the viewing illuminants or given the viewing illuminant spectra in addition to statistics of the reflectance spectra. The results of this work indicate that the use of four color filters could reduce the color errors between the original image and the reproduction well below the just noticeable difference threshold when linear transformations are used to correct the data. In addition, filters derived using statistics for one ensemble of reflectance spectra perform well for other reflectance spectra ensembles.

APPENDIX A
DERIVATION OF MIN/MAX FILTERS

The error term in (9) can be rewritten as

$$\epsilon_l = \underset{\|\mathbf{f}\|^2 \leq 1}{\text{Max}} (\mathbf{f} - \hat{\mathbf{f}})^T \mathbf{S}\mathbf{S}^T (\mathbf{f} - \hat{\mathbf{f}})$$
$$= \underset{\|\mathbf{f}\|^2 \leq 1}{\text{Max}} (\mathbf{f} - \hat{\mathbf{f}})^T \mathbf{B}\mathbf{\Lambda}_S \mathbf{B}^T (\mathbf{f} - \hat{\mathbf{f}}) \tag{32}$$

where $\mathbf{S} = [\gamma_1 \mathbf{O}_1, \gamma_2 \mathbf{O}_2, \ldots, \gamma_K \mathbf{O}_K]$, $\mathbf{S}\mathbf{S}^T = \mathbf{B}\mathbf{\Lambda}_S\mathbf{B}^T$, $\mathbf{\Lambda}_S = \text{Diag}[\lambda_1, \lambda_2, \ldots, \lambda_Q,\ 0, \ldots, 0]$, $\mathbf{B}^T\mathbf{B} = \mathbf{I}_{N\times N}$, Q is the rank of the matrix $\mathbf{S}$, and $\hat{\mathbf{f}}$ is the estimated spectral reflectance calculated from the recorded data. The λ_i's are the squares of the singular values of matrix $\mathbf{S}$. It will be assumed that the λ_i's are ordered so that $\lambda_i \geq \lambda_{i+1}$.

TABLE XIV
COMPARISON OF HVSS FILTERS, THREE OPTIMAL COPIER FILTERS $\gamma_i = 1$, AND THREE WEIGHTED COPIER FILTERS FOR THE COPIER DATA SET WITH COPIER COVARIANCE AND MEAN IN THE LMMSE ESTIMATOR

Illum	Errors	HVSS	3 Filters Copier	3 Filters Copier Weighted
	ΔE_{avg}	3.24	2.76	2.12
A	ΔE_{max}	14.16	11.00	8.20
	$\Delta E \geq 3$	145	121	82
	ΔE_{avg}	0.75	1.43	2.06
D65	ΔE_{max}	2.80	6.92	9.37
	$\Delta E \geq 3$	0	36	80
	ΔE_{avg}	3.08	2.16	2.06
F2	ΔE_{max}	23.48	14.94	12.73
	$\Delta E \geq 3$	110	65	67
	ΔE_{avg}	0.53	1.23	1.85
C	ΔE_{max}	1.94	6.35	8.73
	$\Delta E \geq 3$	0	26	71
	ΔE_{avg}	0.75	1.24	1.91
F7	ΔE_{max}	2.62	4.89	7.62
	$\Delta E \geq 3$	0	21	77
	MSE	$1.53E-3$	$1.30E-3$	$1.44E-3$

TABLE XV
$\Delta E_{L^*a^*b^*}$ VALUES FOR COLOR CORRECTIONS USING THE MUNSELL DATA SET WITH HVSS FILTERS, LMMSE FILTERS, AND PERCEPTUAL FILTERS

Illum	Errors	HVSS	LMMSE	ϵ_{pmse}	ϵ_{pmax1}	ϵ_{pmax2}
	ΔE_{avg}	2.71	1.76	1.67	3.12	2.43
A	ΔE_{max}	8.95	5.65	7.16	4.43	4.05
	$\Delta E \geq 3$	21	8	16	33	16
	ΔE_{avg}	2.17	1.48	0.95	1.57	2.18
F2	ΔE_{max}	9.41	4.86	5.75	2.39	4.05
	$\Delta E \geq 3$	14	6	4	0	16
	ΔE_{avg}	0.72	1.93	1.19	0.49	2.03
D65	ΔE_{max}	2.41	6.70	5.91	2.49	4.05
	$\Delta E \geq 3$	0	12	5	0	14
Illum ΔE_{avg}		1.87	1.72	1.27	2.06	2.21
Illum ΔE_{max}		6.93	5.74	6.28	3.11	4.05

Recall that the product of the recording illuminant $\mathbf{L}_r$ and the color filter matrix $\mathbf{N}$ is the matrix $\mathbf{G} = \mathbf{L}_r\mathbf{N}$. Incorporating the estimate $\hat{\mathbf{f}} = \mathbf{P}_{R(\mathbf{G})}\mathbf{f}$ from (12) into (32), the minimization of ϵ_l with respect to $R(\mathbf{G})$ can be written as

$$\phi = \underset{\substack{R(G)\\ r(G)=P}}{\text{Min}} \underset{\|\mathbf{f}\|^2 \leq 1}{\text{Max}} (\mathbf{f} - \mathbf{P}_{R(\mathbf{G})}\mathbf{f})^T \mathbf{B}\Lambda_S\mathbf{B}^T(\mathbf{f} - \mathbf{P}_{R(\mathbf{G})}\mathbf{f})$$
$$= \underset{\substack{R(G)\\ r(G)=P}}{\text{Min}} \underset{\|\mathbf{f}^2\| \leq 1}{\text{Max}} \mathbf{f}^T(\mathbf{I} - \mathbf{P}_{R(\mathbf{G})})\mathbf{B}\Lambda_S\mathbf{B}^T(\mathbf{I} - \mathbf{P}_{R(\mathbf{G})}\mathbf{f}) \tag{33}$$

where $r(\mathbf{G})$ is the rank of the matrix $\mathbf{G}$. If $\mathbf{x} = \mathbf{P}_{N(\mathbf{G}^T)}\mathbf{f} = (\mathbf{I} - \mathbf{P}_{R(\mathbf{G})})\mathbf{f}$, which is the unique orthogonal projection of $\mathbf{f}$ onto the null space of the matrix $\mathbf{G}^T$, then ϕ can be rewritten as

$$\phi = \underset{\substack{N(\mathbf{G}^T)\\ \nu(\mathbf{G}^T)=N-P}}{\text{Min}} \underset{\substack{\|\mathbf{x}\|^2=1\\ \mathbf{x}\in N(\mathbf{G}^T)}}{\text{Max}} \mathbf{x}^T\mathbf{B}\mathbf{\Lambda}_S\mathbf{B}^T\mathbf{x} \tag{34}$$

where $\nu(\mathbf{G}^T)$ is the dimension of the null space of the matrix $\mathbf{G}^T$. Note that the minimization in (34) is performed with respect to the null space of the matrix $\mathbf{G}^T$, and the maximization includes the constraint that $\mathbf{x} \in N(\mathbf{G}^T)$. From the Courant–Fischer theorem (see pp. 148–149 of [14]), it follows that

$$\phi = \underset{\substack{N(\mathbf{G}^T) \\ \nu(\mathbf{G}^T)=N-P}}{\mathrm{Min}} \ \underset{\substack{\|\mathbf{x}\|^2 \leq 1 \\ \mathbf{x} \in N(\mathbf{G}^T)}}{\mathrm{Max}} \ \mathbf{x}^T \mathbf{B} \mathbf{\Lambda}_S \mathbf{B}^T \mathbf{x} = \lambda_{p+1} \tag{35}$$

where the min/max is achieved when $N(\mathbf{G}^T) = R([\mathbf{b}_{P+1}, \mathbf{b}_{P+2}, \ldots \mathbf{b}_N])$ or equivalently when $R(\mathbf{G}) = R([\mathbf{b}_1, \mathbf{b}_2, \ldots \mathbf{b}_P])$, where the $\{\mathbf{b}_i\}$ are defined in (32).

Appendix B
Derivation of Mean Square Error Filters

The error term in (13) can be rewritten as

$$\epsilon_m = E[(\hat{\mathbf{f}} - \mathbf{f})^T \mathbf{S}\mathbf{S}^T (\hat{\mathbf{f}} - \mathbf{f})] \tag{36}$$

where $\mathbf{S} = [\gamma_1 \mathbf{O}_1, \gamma_2 \mathbf{O}_2, \ldots, \gamma_K \mathbf{O}_K]$ and the estimated spectral reflectance $\hat{\mathbf{f}}$ depends on the color filters and the type of estimator used. Since the ensemble is known, a LMMSE estimator will be used.

The mean of the reflectance spectra is known; therefore, the P-stimulus mean can be removed from the recorded data, and the CIE tristimulus mean for the ensemble under a particular illuminant can be added to the corrected zero-mean data. Since the mean can be removed from the recorded data, it will be assumed for simplicity that the mean of the reflectance spectra ensemble is the zero vector. In the absence of noise, the LMMSE estimate of the reflectance spectra is

$$\hat{\mathbf{f}} = \mathbf{K}_f \mathbf{G}[\mathbf{G}^T \mathbf{K}_f \mathbf{G}]^{-1} \mathbf{G}^T \mathbf{f} \tag{37}$$

where $\mathbf{K}_f$ is the covariance matrix of the reflectance spectra, and the $P \times N$ matrix $\mathbf{G}^T$ is the color filters combined with the recording illuminant, i.e., $\mathbf{G}^T = \mathbf{N}^T \mathbf{L}_r$.

Substituting

$$\mathbf{f} - \hat{\mathbf{f}} = (\mathbf{I} - \mathbf{K}_f \mathbf{G}[\mathbf{G}^T \mathbf{K}_f \mathbf{G}]^{-1} \mathbf{G}^T)\mathbf{f} \tag{38}$$

into (36) and performing algebraic manipulations produces

$$\epsilon_m = \mathrm{Trace}[\mathbf{S}\mathbf{S}^T (\mathbf{K}_f - \mathbf{K}_f \mathbf{G}[\mathbf{G}^T \mathbf{K}_f \mathbf{G}]^{-1} \mathbf{G}^T \mathbf{K}_f)]. \tag{39}$$

To produce a more manageable cost function, the matrix $\mathbf{H} = \mathbf{K}_f^{\frac{1}{2}} \mathbf{G}$ will be substituted into (39) to produce

$$\epsilon_m = \mathrm{Trace}[\mathbf{S}\mathbf{S}^T (\mathbf{K}_f - \mathbf{K}_f^{\frac{1}{2}} \mathbf{H}[\mathbf{H}^T \mathbf{H}]^{-1} \mathbf{H}^T \mathbf{K}_f^{\frac{1}{2}})]. \tag{40}$$

Equation (40) can be rewritten as

$$\epsilon_m = \mathrm{Trace}[\mathbf{S}\mathbf{S}^T \mathbf{K}_f] - \mathrm{Trace}[\mathbf{K}_f^{\frac{1}{2}} \mathbf{S}\mathbf{S}^T \mathbf{K}_f^{\frac{1}{2}} \mathbf{H}[\mathbf{H}^T \mathbf{H}]^{-1} \mathbf{H}^T] \tag{41}$$

from which it is clear that an optimal matrix $\mathbf{H}$, which minimizes ϵ_m, will maximize

$$\zeta = \mathrm{Trace}[\mathbf{K}_f^{\frac{1}{2}} \mathbf{S}\mathbf{S}^T \mathbf{K}_f^{\frac{1}{2}} \mathbf{H}[\mathbf{H}^T \mathbf{H}]^{-1} \mathbf{H}^T]. \tag{42}$$

An orthonormalization of the columns of the matrix $\mathbf{H}_{N \times P}$ can be performed using the Gram–Schmidt process. This will produce a matrix $\mathbf{V}_{N \times P}$ such that $\mathbf{V}^T \mathbf{V} = \mathbf{I}_{P \times P}$ and $\mathbf{H}_{N \times P} = \mathbf{V}_{N \times P} \mathbf{Y}_{P \times P}$, where $Y_{P \times P}$ is nonsingular.

Substituting $\mathbf{H} = \mathbf{V}\mathbf{Y}$ into (42) results in

$$\zeta = \mathrm{Trace}[\mathbf{V}^T \mathbf{K}_f^{\frac{1}{2}} \mathbf{S}\mathbf{S}^T \mathbf{K}_f^{\frac{1}{2}} \mathbf{V}]. \tag{43}$$

The above trace is maximized with respect to the matrix $\mathbf{V}$ when the columns of the matrix $\mathbf{V}$ are the orthonormal eigenvectors associated with the P largest eigenvalues of the matrix $\mathbf{K}_f^{\frac{1}{2}} \mathbf{S}\mathbf{S}_T \mathbf{K}_t^{\frac{1}{2}}$ [13, page 191]. Therefore, the optimal matrix $\mathbf{V}^*$ satisfies

$$\mathbf{K}_f^{\frac{1}{2}} \mathbf{S}\mathbf{S}^T \mathbf{K}_f^{\frac{1}{2}} \mathbf{V}^* = \mathbf{V}^* \Delta \tag{44}$$

where $\mathbf{\Delta} = \mathrm{Diag}[\delta_1, \delta_2, \ldots, \delta_P]$ and $\delta_1 \geq \delta_2 \geq \ldots\ldots \geq \delta_P$.

From the equations $\mathbf{H}^* = \mathbf{V}^* \mathbf{Y}$, $\mathbf{H}^* = \mathbf{K}_f^{\frac{1}{2}} \mathbf{G}^*$, it follows that every matrix $\mathbf{G}$ in the set

$$C_{\mathbf{G}^*} = \{\mathbf{G} | \mathbf{G} = \mathbf{G}^* \mathbf{Y} \ \mathbf{S}\mathbf{S}^T \mathbf{K}_f \mathbf{G}^* = \mathbf{G}^* \mathbf{\Delta} \text{ for some } \mathbf{Y} \in M_p\} \tag{45}$$

minimizes ϵ_m in (13) with respect to $\mathbf{G}$, where M_p denotes the set of $P \times P$ nonsingular matrices.

Appendix C
Filter Sensitivity

If the specified set of filters is denoted by the matrix $\mathbf{G}$ and the perturbation from the set is denoted by $\delta\mathbf{G}$, then the mean square error for the filter set $\mathbf{G} + \delta\mathbf{G}$ is

$$\epsilon_m = E[(\hat{\mathbf{f}} - \mathbf{f})^T \mathbf{S}\mathbf{S}^T (\hat{\mathbf{f}} - \mathbf{f})] \tag{46}$$

where the estimate of $\mathbf{f}$ is

$$\hat{\mathbf{f}} = \mathbf{K}_f(\mathbf{G} + \delta\mathbf{G})[(\mathbf{G} + \delta\mathbf{G})^T \mathbf{K}_f (\mathbf{G} + \delta\mathbf{G})]^{-1} (\mathbf{G} + \delta\mathbf{G})^T \mathbf{f}. \tag{47}$$

It is assumed that the the columns of the matrix $\mathbf{G} + \delta\mathbf{G}$ are linearly independent since linearly dependent filters would not be used for color separation. Following the development of Appendix B by substituting (47) into (46) and using the relationship $\mathbf{H} = \mathbf{K}_f^{\frac{1}{2}} \mathbf{G}$ produces

$$\begin{aligned} \epsilon_m &= \mathrm{Trace}[\mathbf{S}\mathbf{S}^T \mathbf{K}_f] \\ &\quad - \mathrm{Trace}[\mathbf{K}_f^{\frac{1}{2}} \mathbf{S}\mathbf{S}^T \mathbf{K}_f^{\frac{1}{2}} (\mathbf{H} + \delta\mathbf{H})[(\mathbf{H} + \delta\mathbf{H})^T \\ &\quad \times (\mathbf{H} + \delta\mathbf{H})]^{-1} (\mathbf{H} + \delta\mathbf{H})^T] \\ &= \mathrm{Trace}[\mathbf{S}\mathbf{S}^T \mathbf{K}_f] - \zeta \end{aligned} \tag{48}$$

where $\delta\mathbf{H} = \mathbf{K}_f^{\frac{1}{2}} \delta\mathbf{G}$.

Using the relationship $\mathbf{H} = \mathbf{V}\mathbf{Y}$ from Appendix B, where $\mathbf{Y}$ is nonsingular and $\mathbf{V}$ is orthogonal, ζ becomes

$$\begin{aligned} \zeta = \mathrm{Trace}[&\mathbf{K}_f^{\frac{1}{2}} \mathbf{S}\mathbf{S}^T \mathbf{K}_f^{\frac{1}{2}} (\mathbf{V} + \delta\mathbf{V})[(\mathbf{V} + \delta\mathbf{V})^T \\ &\times (\mathbf{V} + \delta\mathbf{V})]^{-1} (\mathbf{V} + \delta\mathbf{V})^T] \end{aligned} \tag{49}$$

where

$$\delta\mathbf{V} = \mathbf{K}_f^{\frac{1}{2}} \delta\mathbf{G}\mathbf{Y}^{-1} \tag{50}$$

and the columns of matrix $\mathbf{V}$ are the P eigenvectors associated with the P largest eigenvalues of the matrix $\mathbf{K}_f^{\frac{1}{2}} \mathbf{S}\mathbf{S}^T \mathbf{K}_f^{\frac{1}{2}}$.

The increase in mean square error introduced by the perturbation is the difference between (43) and (49), which can be written as

$$s = \mathrm{Trace}[(\mathbf{P}_v - \tilde{\mathbf{P}}_v)\mathbf{K}_f^{\frac{1}{2}}\mathbf{S}\mathbf{S}^T\mathbf{K}_f^{\frac{1}{2}}] \tag{51}$$

where $\mathbf{P}_v$ and $\tilde{\mathbf{P}}_v$ are the orthogonal projection operators onto the range spaces of matrix $\mathbf{V}$ and $\mathbf{V} + \delta\mathbf{V}$, respectively. The magnitude of a perturbation can be quantified using the matrix spectral norm. The spectral norm is useful since for a given perturbation matrix $\delta\mathbf{G}$, the spectral norm of that matrix $\|\delta\mathbf{G}\|_2$ is related to the largest error produced by the perturbation. Mathematically, this can be expressed as

$$\operatorname*{Max}_{\|\mathbf{f}\|\leq 1}\|(\mathbf{G} + \delta\mathbf{G})^T\mathbf{f} - \mathbf{G}^T\mathbf{f}\| = \operatorname*{Max}_{\|\mathbf{f}\|\leq 1}\|\delta\mathbf{G}^T\mathbf{f}\| = \|\delta\mathbf{G}^T\|_2.$$

It is of interest to relate the magnitude of the relative perturbation $\frac{\|\delta\mathbf{G}\|_2}{\|\mathbf{G}\|_2}$ to the error s. $\|\mathbf{P}_v - \tilde{\mathbf{P}}_v\|_2$ represents the distance between the subspaces spanned by the ideal filters and the perturbed filters. From [26], a bound on the error $\|\mathbf{P}_v - \tilde{\mathbf{P}}_v\|_2$, given that $\|\delta\mathbf{V}\|_2 < 1$, is

$$\|\mathbf{P}_v - \tilde{\mathbf{P}}_v\|_2 \leq \frac{\hat{\kappa}\frac{\|\mathbf{P}_v^{\perp}\delta\mathbf{G}\|_2}{\|\mathbf{G}\|_2}}{\sqrt{1 + [\hat{\kappa}\frac{\|\mathbf{P}_v^{\perp}\delta\mathbf{G}\|_2}{\|\mathbf{G}\|_2}]^2}} \leq \frac{\hat{\kappa}\frac{\|\delta\mathbf{G}\|_2}{\|\mathbf{G}\|_2}}{\sqrt{1 + \left[\hat{\kappa}\frac{\|\delta\mathbf{G}\|_2}{\|\mathbf{G}\|_2}\right]^2}} \tag{52}$$

where $\mathbf{P}_v^{\perp}$ is the orthogonal projection operator onto the orthogonal complement of the range space of the matrix $\mathbf{V}$

$$\hat{\kappa} = \frac{\sigma_{\max}}{\sigma_{\min}} \tag{53}$$

and $\sigma_{\max}$, $\sigma_{\min}$ are the maximum and minimum singular values of the matrix $\mathbf{G}$. Perturbations for which $\|\delta\mathbf{V}\|_2 \geq 1$ would be large enough to cause the filters to become linearly dependent. A sufficient condition to guarantee that $\|\delta\mathbf{V}\|_2 < 1$ is

$$\|\delta\mathbf{G}\|_2 \leq \frac{1}{\|\mathbf{K}_f^{\frac{1}{2}}\|_2\|\mathbf{Y}^{-1}\|_2}. \tag{54}$$

Consider the effect of the error $\|\mathbf{P}_v - \tilde{\mathbf{P}}_v\|_2$ on s. Using results from p. 183 of [14], the error s is bounded by

$$\begin{aligned} s &= \mathrm{Trace}[(\mathbf{P}_v - \tilde{\mathbf{P}}_v)\mathbf{K}_f^{\frac{1}{2}}\mathbf{S}\mathbf{S}^T\mathbf{K}_f^{\frac{1}{2}}] \\ &\leq \sum_{i=1}^{N}\sigma_i(\mathbf{P}_v - \tilde{\mathbf{P}}_v)\delta_i \leq \|\mathbf{P}_v - \tilde{\mathbf{P}}_v\|_2\sum_{i=1}^{N}\delta_i \\ &= \|\mathbf{P}_v - \tilde{\mathbf{P}}_v\|_2\mathrm{Trace}[\mathbf{K}_f^{\frac{1}{2}}\mathbf{S}\mathbf{S}^T\mathbf{K}_f^{\frac{1}{2}}] \end{aligned} \tag{55}$$

where $\sigma_i(\mathbf{P}_v - \tilde{\mathbf{P}}_v)$ denotes the ith singular value of the matrix $\mathbf{P}_v - \tilde{\mathbf{P}}_v$, and δ_i denotes the ith eigenvalue of the matrix $\mathbf{K}_f^{\frac{1}{2}}\mathbf{S}\mathbf{S}^T\mathbf{K}_f^{\frac{1}{2}}$.

In the above development, the only term that can be controlled is $\hat{\kappa}$. The filters should be specified such that $\hat{\kappa}$ is as small as possible since this will reduce the upper bound on $\|\mathbf{P}_v - \tilde{\mathbf{P}}_v\|_2$ and, hence, the upper bound on the error s. Minimization of $\hat{\kappa}$ can be used as a criteria for the selection of a matrix $\mathbf{Y}$ to enforce the filter nonnegativity constraint (see Section IV).

ACKNOWLEDGMENT

A grant of computer time from the North Carolina Supercomputing Center is gratefully acknowledged.

REFERENCES

[1] K. B. Benson, *Television Engineering Handbook*. New York: McGraw Hill, 1986.

[2] J. D. E. Beyon and D. R. Lamb, *Charge-Coupled Devices and Their Applications*. London: McGraw-Hill, 1980.

[3] L. M. Bregman, "The method of successive projection for finding a common point of convex sets," *Doklady Akademiia Nauk SSSR*, vol. 162, pp. 487–490, 1965. (English translation in *Soviet Mathematics—Doklady*, vol. 6, no. 3, pp. 688–692, 1965).

[4] Y. Chang, P. Liang, and S. Hackwood, "Unified study of color sampling," *Applied Optics*, vol. 28, no. 4, pp. 809–813, Feb. 15, 1989.

[5] J. B. Cohen, "Color and color mixture: Scalar and vector fundamentals," *Color Res. Applications*, vol. 13, no. 1, pp. 5–39, Feb. 1988.

[6] J. B. Cohen and W. E. Kappauf, "Metameric color stimuli, fundamental metamers and Wyszecki's metameric blacks," *Amer. J. Psych.*, vol. 95, no. 4, pp. 537–564, Winter 1982.

[7] ——, "Color mixture and fundamental metamers: theory, algebra, geometry, application," *Amer. J. Psych.*, vol. 98, no. 2, pp. 171–259, Summer 1985.

[8] J. E. Dennis and R. B. Schnabel, *Numerical Methods for Unconstrained Optimization and Nonlinear Equations*. Englewood Cliffs, NJ: Prentice-Hall, 1983.

[9] G. H. Golub and C. F. Van Loan, *Matrix Computations*. Baltimore, MD: John Hopkins University Press, 1989, 2nd ed.

[10] F. Grum and R. J. Becherer, *Optical Radiation Measurements: Volume 1. Radiometry*. New York: Academic, 1979.

[11] M. Herbin, A. Venot, J. Y. Devaux, and C. Piette, "Color quantitation through image processing in dermatology," *IEEE Trans. Med. Imaging*, vol. 9, no. 3, pp. 262–269, Sept. 1990.

[12] B. K. P. Horn, "Exact reproduction of colored images," *Comput. Vision Graphics Image Processing*, vol. 26, pp. 135–167, 1984.

[13] R. A. Horn and C. R. Johnson, *Matrix Analysis*. Cambridge: Cambridge University Press, 1985.

[14] R. A. Horn and C. R. Johnson, *Topics in Matrix Analysis*. Cambridge: Cambridge University Press, 1991.

[15] G. H. Jacobs, *Comparative Color Vision*. New York: Academic, 1981.

[16] R. V. Kollarits and D. C. Gibbon, "Improving the color fidelity of cameras for advanced television systems," *SPIE Proc.*, vol. 1656, 1992.

[17] D. G. Luenberger, *Introduction to Linear and Nonlinear Programming*. Reading, MA: Addison-Wesley, 1984, 2nd ed.

[18] A. Lyons and E. Buckner, "Color aerial photography detects nutrient status of loblolly pine plantations," in *Proc. 8th Biennial Workshop Color Aerial Photo. Plant Sci. Related Fields*, Apr. 1981, pp. 53–58.

[19] D. H. Marimont and B. A. Wandell, "Linear models of surface and illuminant spectra," *J. Opt. Soc. Amer. A*, vol. 9, no. 11, pp. 1905–1913, Nov. 1992.

[20] K. Martinez, J. Cupitt, and D. Saunders, "High resolution colorimetric imaging of paintings," *SPIE Proc.*, vol. 1901, 1993.

[21] W. K. Pratt, *Digital Image Processing*. New York: Wiley, 1991, 2nd ed.

[22] B. D. Rao, "Perturbation analysis of an SVD-based linear prediction method for estimating the frequencies of multiple sinusoids," *IEEE Trans. Acoust. Speech Signal Processing*, vol. 36, pp. 1026–1035, July 1988.

[23] N. R. Sarkar, "Images: From a printer's perspective," *SPIE Proc.*, vol. 1458, 1991.

[24] F. T. Simon, "Principles of color sorting," *AATCC-ISCC Symp. Practical Applications Color Contr.*, 1983, pp. 22–24.

[25] S. Stamm, "An investigation of color tolerance," in *TAGA Proc. 1981*, pp. 156–173.

[26] G. W. Stewart, "On the perturbation of pseudo-inverses, projections and linear least squares problems," *SIAM Rev.*, vol. 19, no. 4, pp. 634–662, Oct. 1977.

[27] M. Stokes, M. D. Fairchild, and R. S. Berns, "Precision requirements for digital color reproduction," *ACM Trans. Graph.*, vol. 11, no. 4, pp. 406–422, Oct. 1992.

[28] M. C. Stone, W. B. Cowan, and J. C. Beatty, "Color gamut mapping and the printing of digital color images," *ACM Trans. Graph.*, vol. 7, no. 3, pp. 249–292, Oct. 1988.

[29] S. Suzuki, T. Kusunoki, and M. Mori, "Color characteristic design for color scanners," *Applied Opt.*, vol. 29, no. 34, pp. 5187–5192.

[30] H. J. Trussell "Applications of set theoretic methods to color systems," *Color Res. Application*, vol. 16, no. 1, pp. 31–41, Feb. 1991.
[31] P. L. Vora, H. J. Trussell, and L. Iwan, "A mathematical method for designing a set of colour scanning filters," *Proc. SPIE*, vol. 1912, 1993.
[32] M. J. Vrhel and H. J. Trussell, "Color correction using principal components," *Color Res. Application*, vol. 17, no. 5, pp. 328–338, Oct. 1992.
[33] B. A. Wandell, "The synthesis and analysis of color images," *IEEE Trans. Patt. Anal. Machine Intell*, vol. PAMI-9, no. 1, pp. 2–13, Jan. 1987.
[34] W. D. Wright, "The measurement of colour," published in *Vision and Visual Dysfunction*. vol. 6 of *The Perception of Colour* (Peter Gouras Ed.). Boca Rotan, FL: CRC, 1991.
[35] G. Wyszecki and W. S. Stiles, *Color Science: Concepts and Methods. Quantitative Data and Formulae*. New York: Wiley, 1982, 2nd ed.
[36] G. Wyszecki, *Color in Business, Science and Industry* . New York: Wiley, 1975, 3rd ed.
[37] H. Zollinger, "The importance of colour vision for man," in *Food Acceptance and Nutrition*. London: Academic, 1987.

Michael J. Vrhel (M'94) was born in St. Joseph, MI, in 1964. He received the B.S. degree in electrical engineering from Michigan Technological University, Houghton, MI, in 1987. He received the M.S. and Ph.D. degrees in electrical engineering from North Carolina State University, Raleigh, in 1989 and 1993, respectively.

He was the recipient of a Kodak Fellowship from Eastman Kodak Company, Rochester, NY, from 1989 to 1993. During 1992, he researched problems in color reproduction, signal restoration/reconstruction, and optimization methods.

Dr. Vrhel is an associate member of Sigma Xi and a member of Pi Mu Epsilon.

H. Joel Trussell (SM'91–F'94) was born in Atlanta, GA, on February 3, 1945. He received the B.S. degree from the Georgia Institute of Technology, Atlanta, in 1967, the M.S. degree form Florida State University, Gainesville, in 1968, and the Ph.D. degree from the University of New Mexico, Albuquerque, in 1976.

He joined the Los Alamos Scientific Laboratory, Los Alamos, NM, in 1969, where he began working on image and signal processing in 1971. During 1978–1979, he was a visiting professor at Heriot-Watt University, Edinburgh, Scotland. In 1980, he joined the Electrical and Computer Engineering Department at North Carolina State University, Raleigh. During 1988–1989, he was a visiting scientist at the Eastman Kodak Company, Rochester, NY. His current interests include signal restoration/reconstruction, color reproduction, and mathematical methods.

Dr. Trussell has won the IEEE-ASSP Society Senior Paper Award (with M. R. Civanlar). He has been an Associate Editor for the IEEE TRANSACTIONS ON ACOUSTICS, SPEECH AND SIGNAL PROCESSING and a member and chairman of the Image and Multidimensional Digital Signal Processing Committee of that Society. He is a member of Sigma Xi, Tau Beta Pi, Phi Kappa Phi, and the Signal Processing Society.